KANSAS GEOLOGICAL SURVEY
OPEN-FILE REPORT 84-17

A COMPREHENSIVE GEOPHYSICAL INTERPRETATION OF THE MIDCONTINENT GEOPHYSICAL ANOMALY

IN NORTHEATERN KANSAS

by

Chaturong Somanas

Disclaimer

The Kansas Geological Survey does not guarantee this document to be free from errors or inaccuracies and disclaims any responsibility or liability for interpretations based on data used in the production of this document or decisions based thereon. This report is intended to make results of research available at the earliest possible date, but is not intended to constitute final or formal publications.

Kansas Geological Survey
1930 Constant Avenue
University of Kansas
Lawrence, KS 66047-3726

A COMPREHENSIVE GEOPHYSICAL INTERPRETATION OF THE MIDCONTINENT GEOPHYSICAL ANOMALY IN NORTHEASTERN KANSAS

by

Chaturong Somanas
B.S., Mahidol University, Thailand, 1975

Submitted to the Department of Physics and the Faculty of the Graduate School of the University of Kansas in partial fulfillment of the requirements for the degree of Master of Science.

Professor in Charge

Committee Members

For the Department

ACKNOWLEDGEMENTS

I would like to express my deep gratitude to Dr. Ralph Knapp and Dr. Harold Yarger for their excellent guidance in reprocessing the seismic data and modeling the potential fields data, respectively, as well as their consistent encouragement and patience throughout. I am really grateful to Dr. Don Steeples for his valuable advice toward this study and his continued support, both financially and psychologically, without which this thesis is impossible.

Many thanks to Dr. Thomas Armstrong who gave valuable comments, and to Dr. Pat Bickford for the discussion which was indispensible.

I also would like to acknowledge the staff of the Kansas Geological Survey, especially the gravity and aeromagnetic crews for gathering and processing the data, and Dr. Harold Yarger and Al Martin for the computer programs of potential fields modeling and paleopoles calculation. Thanks to Shlomo Shmuelov for the assistance in handling COCORP seismic data.

Finally, I extend my sincere appreciation to my wife, Marissa, for continually encouraging and supporting me.

ABSTRACT

A geophysical model of the Midcontinent Geophysical Anomaly (MGA) in northeastern Kansas is derived to fit gravity and magnetic data using an initial model suggested from COCORP seismic sections, combined with available drill data. An asymmetric basin filled with interbedded basaltic and clastic rocks at shallow crust is mainly responsible for the primary positive magnetic anomaly of the MGA. The favorable direction of net magnetization indicates that the remnant magnetization is significant with an estimated Q value of 1.

The presence of deeper mafic intrusion, with low magnetic effects, at midcrustal levels and extending to the deep crust is required in order to match the positive gravity anomaly. Nonmagnetic Rice Formation basins of low density on both sides of the MGA are proposed to fit the flanking lows of the gravity anomaly.

Reprocessing part of COCORP seismic data reveals a possible mafic intrusion in the shallow crust beneath a secondary magnetic high. According to its magnetization direction determined from magnetic modeling, paleopoles studies support its younger age compared to the central basaltic rift basin. Because it has a cross-cutting relationship with the Rice Formation, it is younger than the Rice Formation.

TABLE OF CONTENTS

LIST OF ILLUSTRATIONS

INTRODUCTION

The Midcontinent Geophysical Anomaly (MGA) is a zone of pronounced positive gravity anomalies averaging 60 km wide with flanking gravity lows (figure 1) and associated magnetic highs, which extend from Lake Superior over 1000 km southerly to Kansas (King and Zietz, 1971) and into Oklahoma (Yarger, 1981). It is generally inferred to be related to an aborted continental rift in late Precambrian time (Chase and Gilmer, 1973; Ocola and Meyer, 1973). Exposures of Keweenawan mafic igneous and sedimentary rocks in the Lake Superior region provide a locality for both geological and geophysical investigations (Halls, 1966 and 1978; White, 1966). This area serves as a model for interpretation of gravity and magnetic anomalies further south where the Precambrian crust is entirely covered by Phanerozoic sediments.

The purpose of this study is to investigate the geophysical model responsible for the MGA in northeastern Kansas using information from the area including gravity data (Yarger and others, 1980), aeromagnetic data (Yarger and others, 1981), and COCORP (Consortium for Continental Reflection Profiling) seismic data (Serpa and others, 1984; Brown and others, 1983). Drilling to the basement in this area also

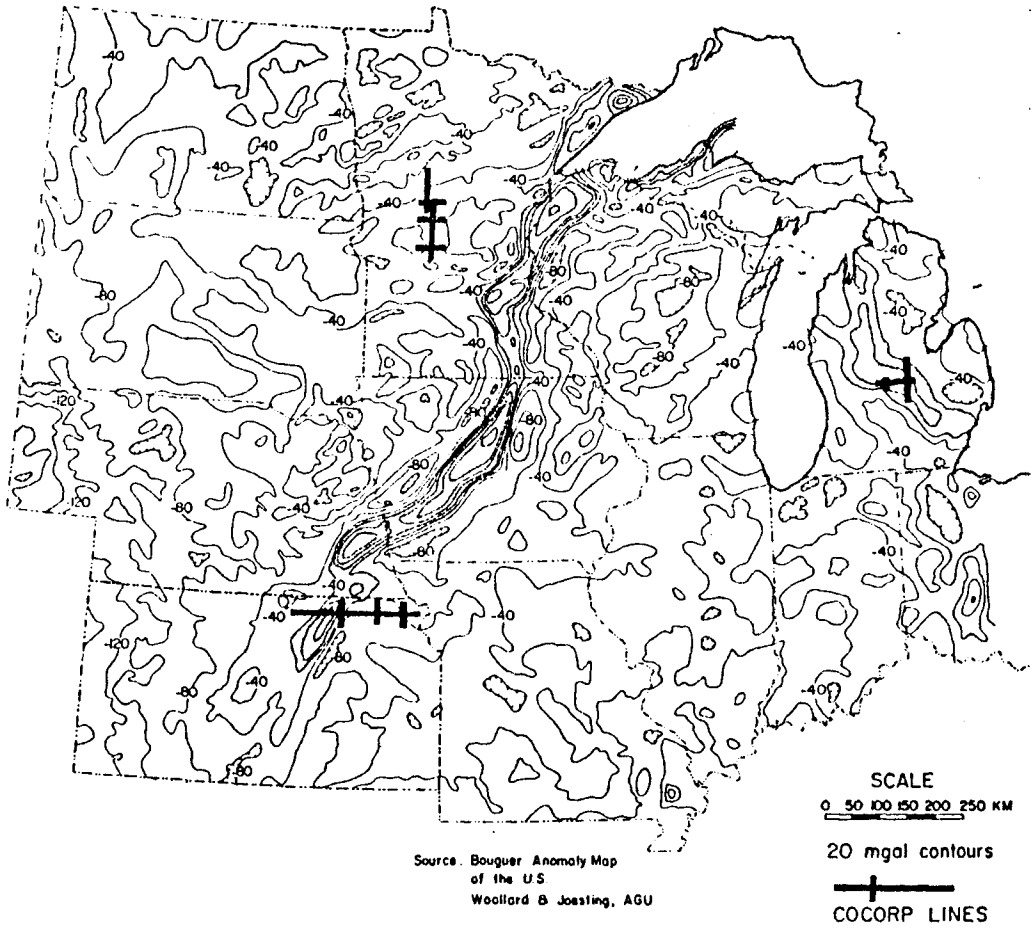

Figure 1. Bouguer gravity map of the midcontinent (After Woolard and Joesting, 1964 in Serpa and others, 1984) with the COCORP seismic lines.

provides generalized geologic information of the uppermost Precambrian crust (Bickford and others, 1979).

The initial model suggested from the COCORP seismic sections is tested against the observed gravity and magnetic data through potential fields modeling. This improves the model shape and expands available information on density and net magnetization of the model.

Reprocessing part of COCORP seismic data is done along the 10 km long east-west profile on the east side of the MGA. Seismic sections of improved quality in this area are needed in order to interpret the corresponding gravity and magnetic anomaly, especially the secondary magnetic anomaly high which trends along the southeastern flank of the MGA. Finally, the derived model is improved by requiring correspondence with the gravity and magnetic data.

This geophysical model illustrates correlations of gravity, magnetic, and seismic data along with drill hole information. The simultaneous use of these data sets should yield a more reliable geologic and tectonic model of this ancient continental rift.

GEOLOGICAL AND GEOPHYSICAL BACKGROUND

In Kansas, Precambrian basement rocks are entirely covered by a relatively thin veneer of Phanerozoic sediments. The region has not been significantly deformed since at least late Paleozoic time, and therefore is part of the Central Stable Region in the Midcontinent (Snyder, 1968). However, with regards to several prominent basement structures such as the late Precambrian rift associated with the MGA, the Nemaha ridge, and the Central Kansas Uplift (figure 2), its geologic history is more complex than the simplicity of flat-lying beds. Microearthquake activity, indicating the possible active fault trends, mainly lies along the same structural trend of these major basement structures (figure 3) (Steeples and others, 1983).

The Nemaha Ridge is a linear trend of basement uplift in eastern Kansas parallel to the MGA. It was intermittently active during Paleozoic time separating the Forest City and Salina basins (Merriam, 1963). It is bounded on the eastern flank by the Humboldt Fault Zone which has microearthquake activity (Steeples and others, 1979). Based on drill data (Cole, 1976), the crystalline basement rocks on the western side are upthrown to within 200 meters of the surface in the area of study. Along the ridge, basement granitic rocks are

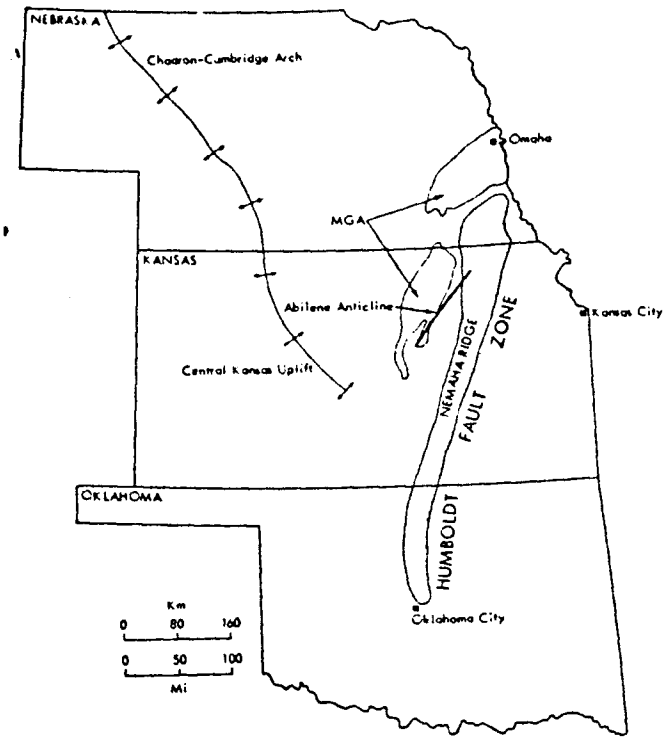

Figure 2. Regional structural uplifts in Kansas vicinity. (From Steeples and Bickford, 1981).

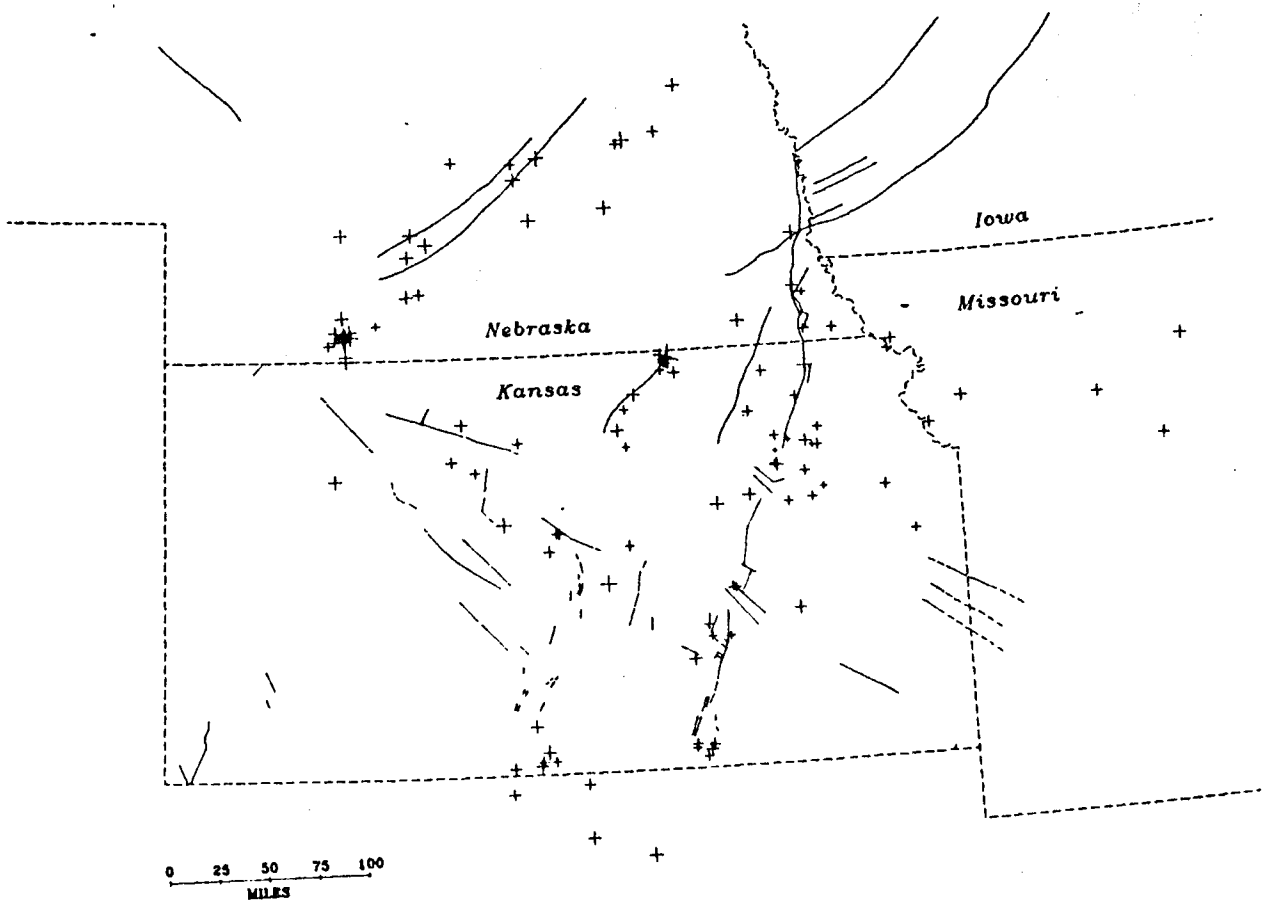

Figure 3. Microearthquakes located by Kansas and Nebraska networks since August, 1977. Locations are shown by '+' and are size coded. (After Steeples and others, 1983).

mostly cataclastically deformed, indicative of a major crustal fracture zone (Bickford and others, 1979).

Between and subparallel to both the MGA and the Nemaha Ridge is the Abilene anticline, a secondary basement uplift of possibly similar age to the Nemaha Ridge and Central Kansas Uplift (Jewett, 1941; Shenkel, 1959). Along the same structural trend of the Abilene anticline there are exposures of the Upper Cretaceous kimberlite intrusive rocks in Riley County (Brookins, 1970). Chelikowsky (1972) suggested they are related to right lateral strike-slip on a fault buried along the east flank of the Abilene anticline. However, their origin is still in doubt because the long axis of intrusions is perpendicular, instead of parallel, to the axis of the Abilene anticline (Steeples, 1982, pp. 58-59).

The Central Kansas Uplift is a northwesterly trend of basement uplift which formed the southern and western boundary of the Salina basin. Its trend does not suggest a relationship to the MGA, the Nemaha Ridge, and the Abilene anticline, but this possibility cannot be completely ruled out without further information.

The distribution of Precambrian basement rocks within the uppermost crust is inferred primarily from shallow basement well samples and geophysical data. In

northern Kansas, except in the area of the MGA, the basement terrane is dominated by 1.6 b.y. old mesozonal granite (Bickford and others, 1981; Bickford and others, 1979) containing isolated intrusions of 1.3 b.y. old epizonal granite (Steeples and Bickford, 1981; Yarger, 1983). The younger basement terrane in southern Kansas is characterized by 1.4 b.y. old epizonal granite and silicic volcanic rocks (Bickford and others, 1981). This seems to suggest that geologic events during late Precambrian time included extensive periods of igneous activity (Snyder, 1968). The last major period of igneous activity correlates with the development of the initial stages of a continental rift. The MGA is the geophysical expression of this aborted rift.

In Kansas, within the trend of the MGA, mafic igneous and arkosic sedimentary rocks are encountered in basement wells (Bickford and others, 1979) (figure 4). These rocks are generally inferred to be related to the exposed 1.1 b.y. old Keweenawan mafic igneous and associated sedimentary rocks in the Lake Superior region. This is based on the lithologic similarity and the geophysical continuity of gravity and magnetic data from Kansas to that area (King and Zietz, 1971).

The Keweenawan geology of the Lake Superior region is reviewed by Halls (1966). There are three

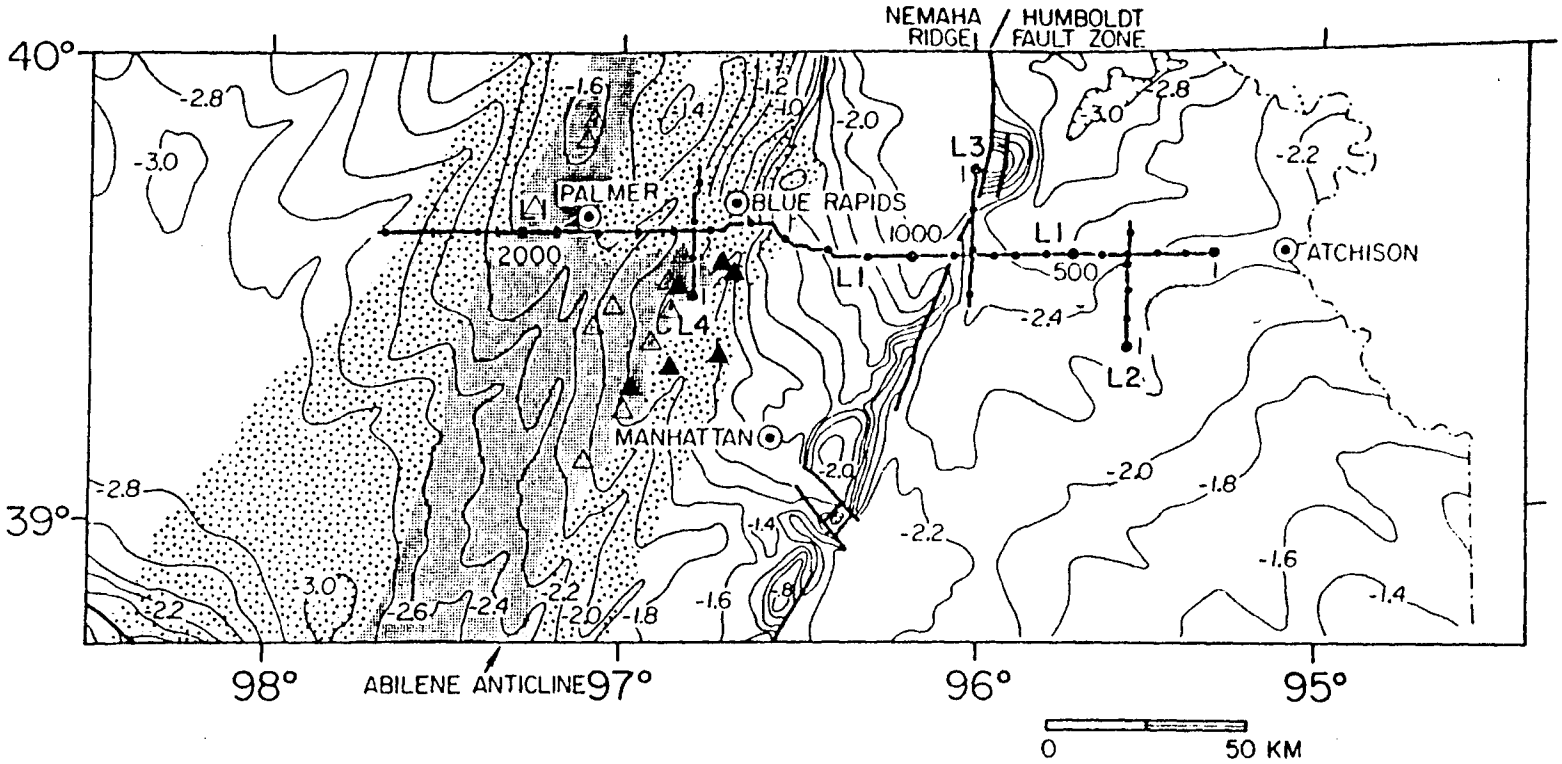

Figure 4. Structural contours (in kilofeet) at top of the Precambrian basement in northeastern Kansas (after Cole, 1976). Dark shading shows the inferred extent of mafic rocks and dots area represents the Rice formation (after Bickford and others, 1979). △ = Olivine-bearing gabbroic rocks (Bickford, personal communication, 1984).
▲ = Riley County kimberlites (Brookins, 1970).
Location of COCORP profiles are shown with vibration points. (From Brown and others, 1983).

lithological divisions for Keweenawan rocks: the Lower Keweenawan of reversely magnetized sediments, the Middle Keweenawan of normally magnetized basaltic lavas with interbedded sediments, and the Upper Keweenawan of normally magnetized fine-grained sandstones and shales overlying a thick conglomerate. Keweenawan intrusions of sills, dikes, and irregular bodies of generally basaltic composition are abundant in the Lake Superior region. It is inferred that igneous activity during Keweenawan time was characterized by an episode of volcanism and subsequent intrusions, where volcanism was punctuated by short pauses that allowed formation of thin interflow sediments (Halls, 1978). In the Lake Superior region, an enormous quantity of basic volcanics is estimated to exist. At the end of igneous activity, subsidence of the mafic rift basin followed and allowed the deposition of a thick sequence of conglomerates and sandstones.

In a preliminary result of a study of thin sections from basement well samples Bickford and others (1979) reported mafic rocks, in Kansas, of mostly olivine-bearing gabbroic rocks. Seven of the twelve wells that encountered mafic rocks lie along the southeastern flank of the MGA (Bickford, personal communication, 1984).

Precambrian arkosic rocks and siltstones in Kansas

comprise the Rice Formation (Scott, 1966). They were apparently formed from immature sediments derived from the faulted edges of the rift basin and deposited within it. Sedimentary rock is usually considered to be of relatively low density and nonmagnetic compared to mafic rock. Therefore, the presence of Rice Formation basins surrounding the mafic igneous rift basin can be inferred from the flanking lows of the gravity anomaly. Also, analysis of aeromagnetic data in Kansas have shown a magnetic quiet zone, where the Rice formation is suspected, surrounding the magnetic high of the MGA (Yarger, 1983) (figure 5).

Earlier work using gravity and magnetic modeling of the MGA in northeastern Kansas was done by Yarger (1980, in Hahn, 1980) and is shown in figure 6. Analysis of teleseismic (Hahn, 1980) and microearthquake waves arriving in eastern Kansas (Lui,1981; Miller, 1983) also suggests the presence of a high velocity crustal body beneath the MGA relating to the mafic igneous body. Miller (1983) also suggests the existence of a low velocity crustal body on the northwest flank of the MGA which is possibly related to the arkosic sedimentary Rice Formation.

Recently, deep seismic reflection data from COCORP across the MGA in northeastern Kansas revealed a thick

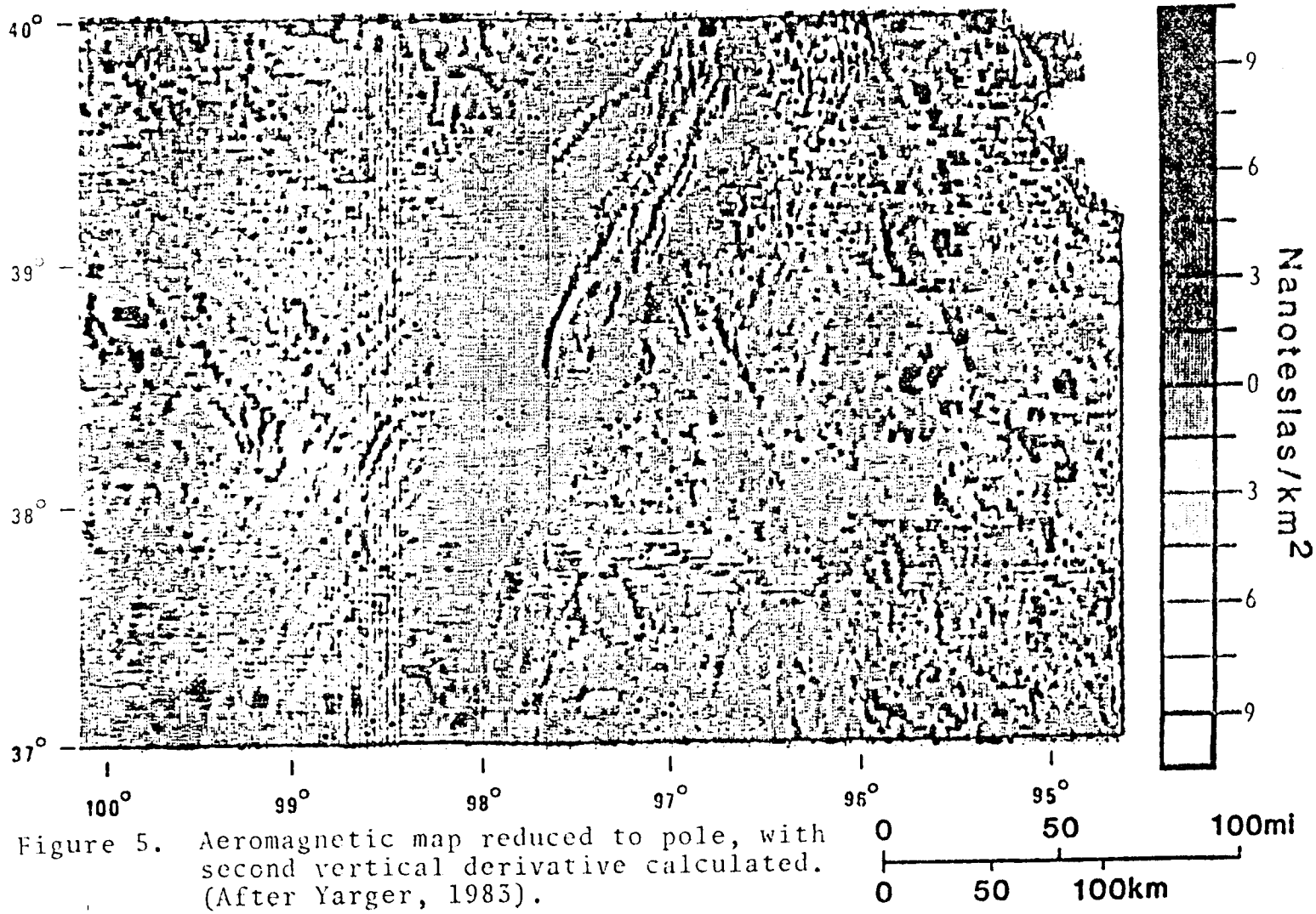

Figure 5. Aeromagnetic map reduced to pole, with second vertical derivative calculated. (After Yarger, 1983).

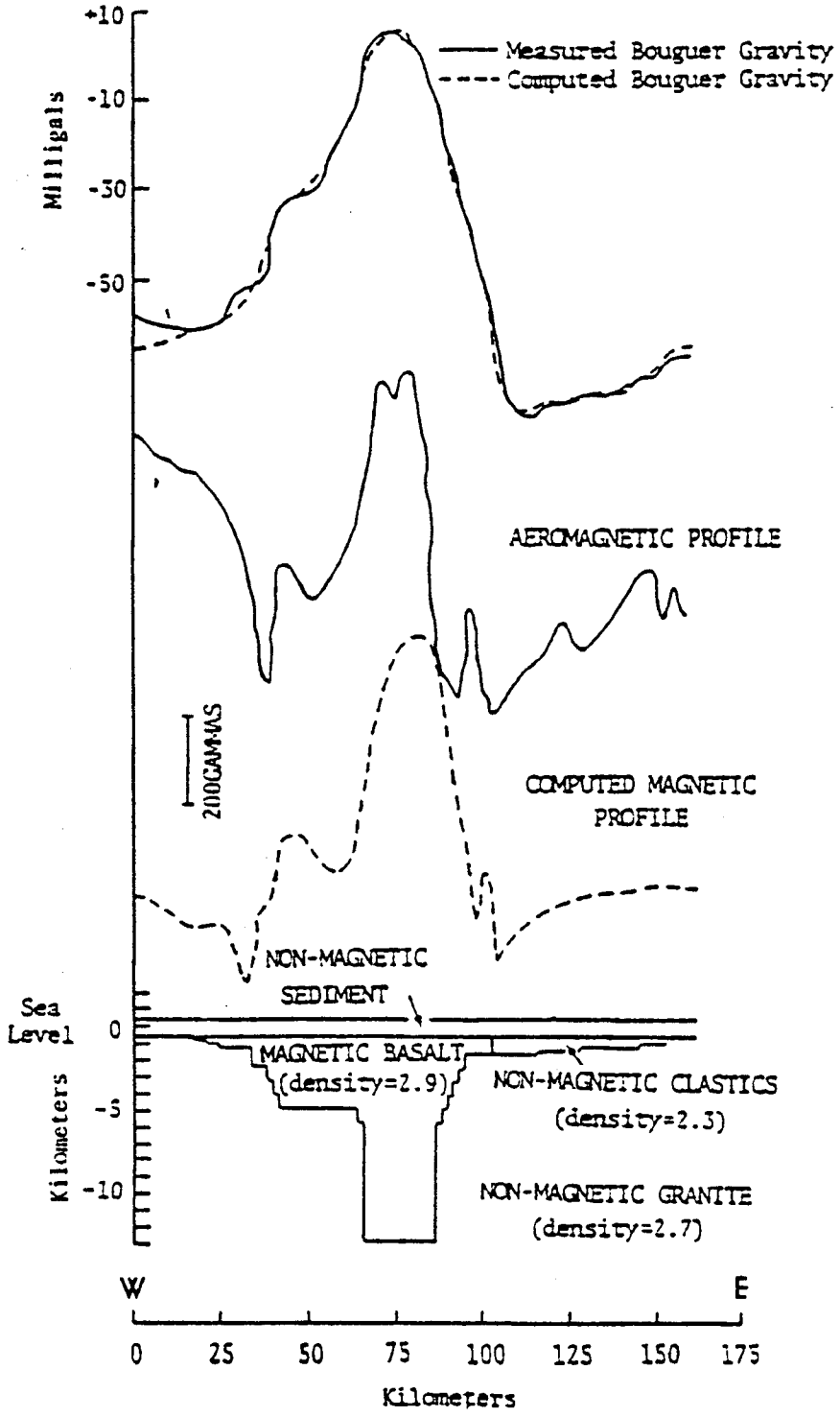

Figure 6. Gravity and magnetic modeling across the MGA from 96.15° to 98.0° W longitude at 39.5° N latitude. Density is in gm/cm^3. (After Yarger, 1980, in Hahn, 1980).

layered wedge of moderately west-dipping strong reflections grading upward into a zone of weak reflections beneath the base of Paleozoic strata (Serpa and others, 1984) (figure 7). It is interpreted as being a highly asymmetric basin filled with the Middle Keweenawan Unit of interbedded basalt and clastic rocks grading upward into the Upper Keweenawan Unit of late Precambrian sedimentary rocks. The rift basin is bounded by asymmetric faults, a result of block rotation during crustal extension. Its dimensions are approximately 40 km east-west wide and about 8 km deep, with its center at the gravity maxima. Gravity modeling calls for the existence of a deeper mafic intrusion beneath the rift basin (Serpa, personal communication, 1984).

From preliminary COCORP results in northeastern Kansas (Brown and others, 1983), except in the MGA area, the generalized picture of the continental crust beneath the Paleozoic strata is that of a shallow crustal zone relatively free of reflections, a midcrustal zone with numerous reflections and diffractions, and a transition zone of rapid decrease in reflections at the expected arrival time of the Moho-discontinuity. However, beneath the MGA area the mid-crustal reflections and diffractions are absent. This unusual midcrustal zone

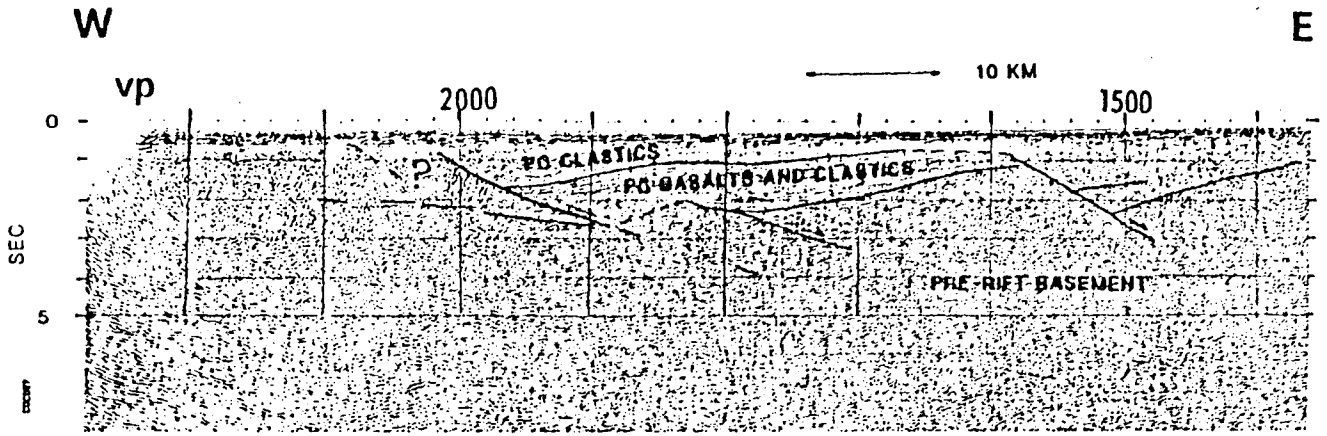

Figure 7. COCORP seismic section (migrated) across the MGA from VP 1360 to VP 2334, interpreted by Serpa and others (1984).
(From Serpa and others, 1984).

may be related to the presence of deep mafic intrusions beneath the MGA, as required from the gravity modeling by Serpa (personal communication, 1984).

A seismic refraction study in northwestern Kansas combined with the regional gravity gradient (Steeples, 1976) indicates a gently west dipping Moho at about 34-38 km deep in north-central Kansas. Hahn (1980), Lui (1981), and Miller (1983), based on analysis of earthquake waves, also independently predicted an anomalously low velocity body in the upper mantle beneath the MGA due to the delay of seismic waves across the MGA as they travel along the top of the mantle.

POTENTIAL FIELDS

Gravity Data

Bouguer gravity data in northeastern Kansas have been compiled by Yarger and others (1980) (figure 8). Most of these data were acquired by the Kansas Geological Survey using a Worden gravimeter of ±0.01 mgal sensitivity. In the area of study, the measurement pattern was an east-west traverse with 1.6 to 3.2 km (1 to 2 miles) spacing between stations and a north-south spacing of 6.4 to 9.6 km (4 to 6 miles) between traverses. Field work procedures were generally similar to more recent gravity surveys in other parts of the state described by Yarger and Lam (1982).

A base station was established for each divided survey area and was tied to a nearby Department of Defense base station (the International Gravity Standardization Net 1971), which permitted the determination of absolute gravity values. In daily work, repeated base station readings were used for correction of the earth's tidal variation and meter drift. Meter drift is expected to be approximately linear within a period of 3-4 hours. However, a somewhat nonlinear drift sometimes occurred because of poor temperature compensation in the Worden gravimeter

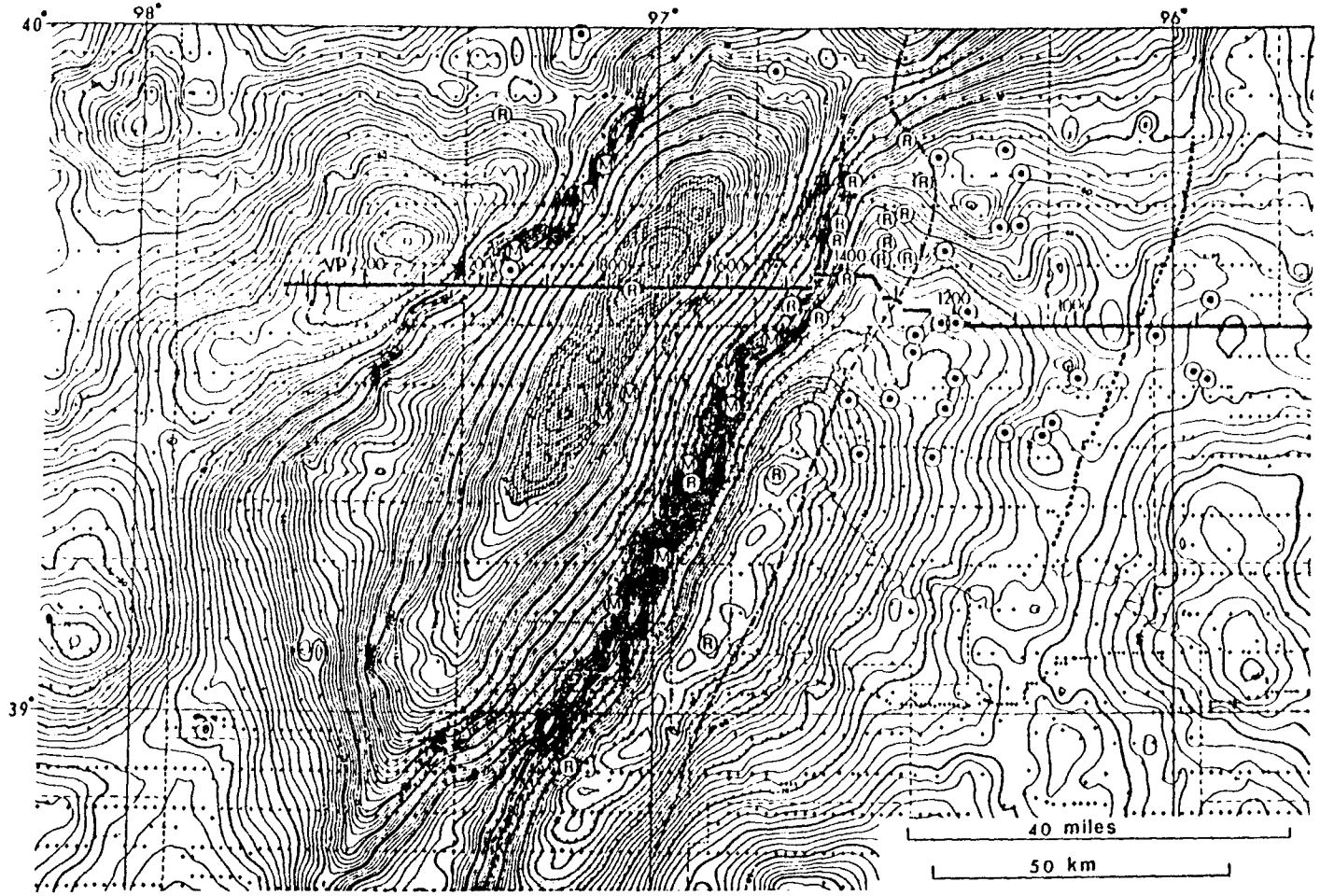

Figure 8. Bouguer gravity map of northeastern Kansas (contour interval 1 milligal) (Yarger and others, 1980) with an east-west COCORP seismic line. Drill data (Bickford, personal communication, 1984):
Ⓜ = Mafic rocks, Ⓡ = Rice formation, ⊙ = Granites,
—·—·—·— = Inferred boundary between Rice formation and granites.
•••••••••• = Humboldt fault zone.

(Yarger and Jarjur, 1972, p. 6). In northeastern Kansas the estimated station measurement error is 0.3 mgal (Yarger and others, 1980).

The Gravity Formula 1967 for the reference spheroid (see for example, Telford and others, 1976, p. 15), which is a function of latitude, was calculated at each measurement location and subtracted from the measured gravity field. Terrain corrections were not required because of the low relief topography in Kansas. Bouguer gravity values were calculated at sea level using a density of 2.67 gm/cm^3.

These final corrected data were then gridded into 1.6 km by 1.6 km (1 mile by 1 mile) nodes using a computer contouring program. The root-mean-square difference between the final corrected data and the interpolated grid values was similar to recent work for southeastern Kansas data (Yarger and Lam, 1982) which is approximately 0.5 mgal. The accuracy of these gridded data is adequate for gravity modeling in this study since the anomaly amplitude of the MGA in the area of study is about 100 mgal. In the potential field modeling which follows, calculations were made at 1.6 km (1 mile) intervals along the east-west profile.

The east-west gravity profiles of gridded data across the MGA are shown in figure 9, where solid lines

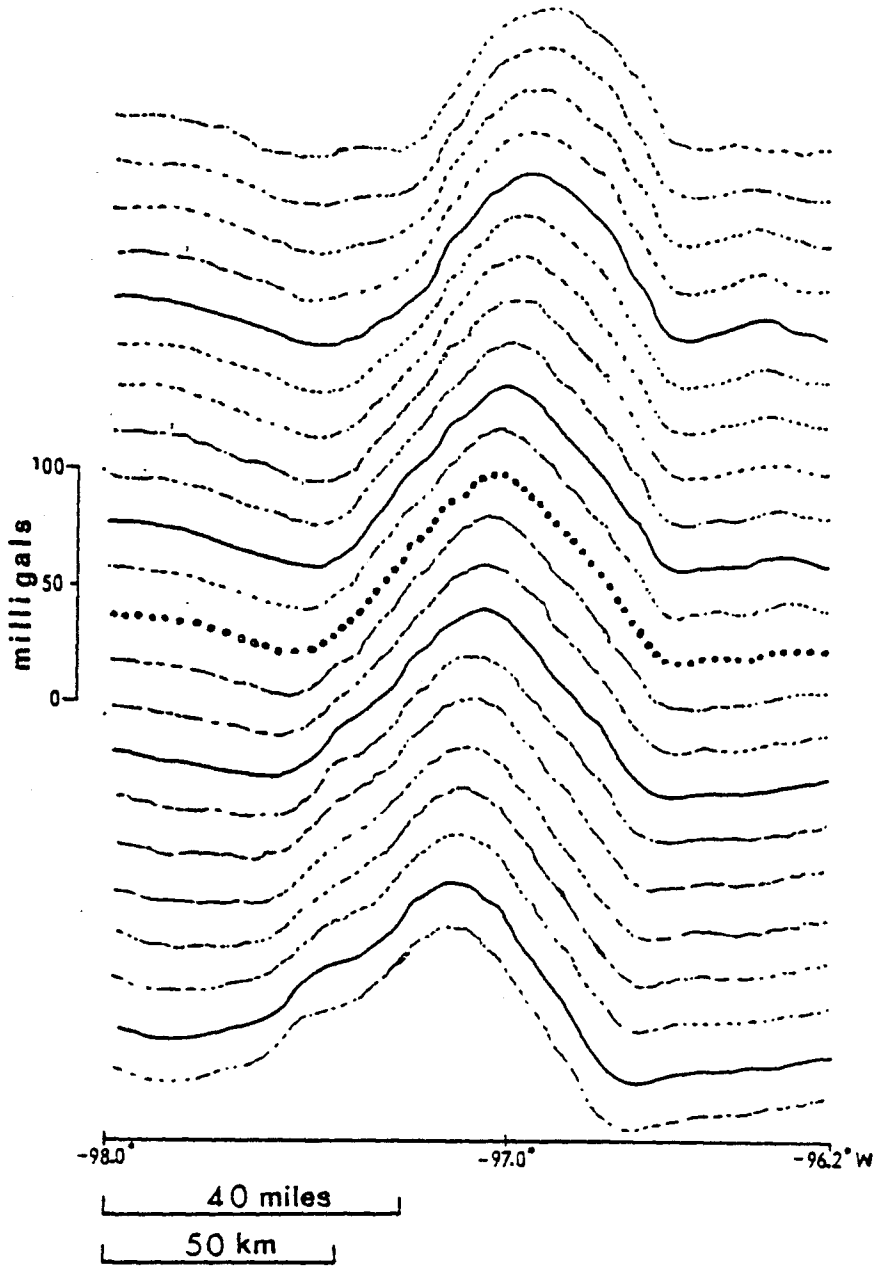

Figure 9. East-west gravity profiles across the MGA.
North-south spacing between adjacent profiles is 1 mile.
———— Profiles close to measurement station.
---------- Interpolated profiles.
•••••••••• Profile close to COCORP east-west line
(at 39.623° N latitude).

are the anomaly profiles close to the original measurement profiles in the MGA area. The profile used in gravity modeling is chosen closest to the east-west COCORP seismic line which is across the MGA at 39.625 N latitude. The anomaly amplitude is 82 mgal, where the high level is at 8 mgal with a flanking low of -74 mgal.

Aeromagnetic Data

The aeromagnetic survey in Kansas was completed by the Kansas Geological Survey in 1979. The relative total intensity of the magnetic field in northeastern Kansas is shown in figure 10 (Yarger and others, 1981). Details in data acquisition and data reduction, along with regional interpretation of aeromagnetic data, are described by Yarger (1983). Measurements of the total intensity of the earth's magnetic field were taken using a proton precession magnetometer of ±1 gamma sensitivity.

In eastern Kansas, the flight elevation was 760 meters above sea level. The flight lines were spaced 3.2 km (2 miles) apart and the tie lines were spaced 32 km (20 miles) apart. The temporal variation in magnetic field (diurnal drift) was removed by analysis of the mismatches of magnetic field values at the tie line-flight line intersections (Yarger and others, 1978). This procedure does not require a recording base station and assumes the diurnal drift during flight to be a smoothly varying low order polynomial in time. The procedure is therefore valid during a magnetically quiet day where magnetic variation is smooth, regular and low in amplitude. Care was taken to cancel the flight on days of severe magnetic fluctuation.

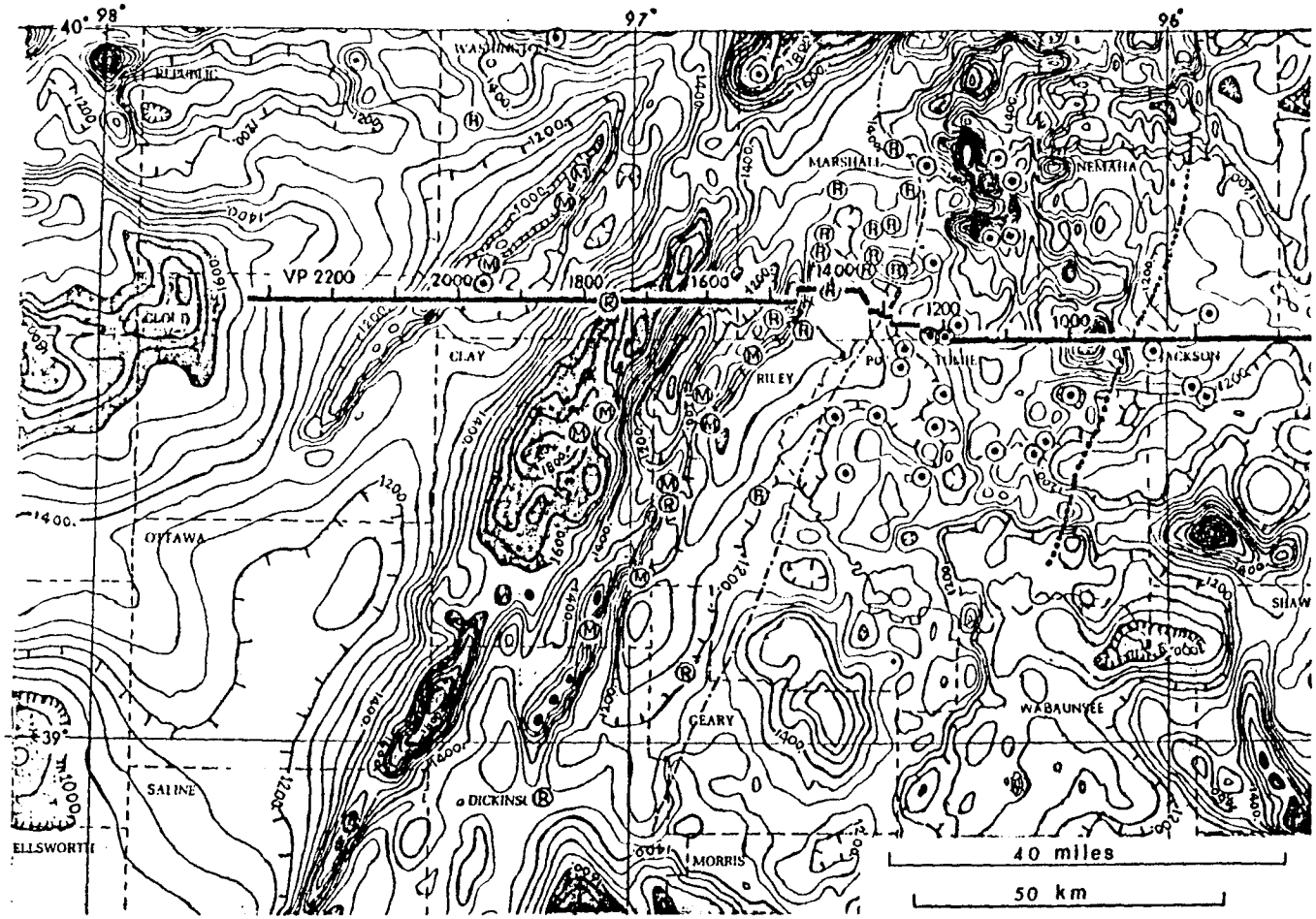

Figure 10. Aeromagnetic map of northeastern Kansas (contour interval 50 gammas) (Yarger and others, 1981), with an east-west COCORP seismic line. Drill data (Bickford, personal communication, 1984): Ⓜ = Mafic rocks, Ⓡ = Rice formation, ⊙ = Granites,
—·—·—·— = Inferred boundary between Rice formation and granites.
····· = Humboldt fault zone.

The International Geomagnetic Reference Field 1975 was computed at each measurement location at the appropriate day and subtracted from the measured total-intensity-magnetic field. The resulting data represent the relative total intensity of the earth's magnetic field. These data were then gridded at a 0.16 km (0.1 mile) east-west spacing and 3.2 km (2 miles) north-south spacing, which is nearly equivalent to the original measurement spacing. From this initial fine grid the 1.6 km by 1.6 km (one mile by one mile) gridded data were generated and are shown in figure 11 as east-west profiles across the MGA, where solid lines represent profiles close to the original measurement profiles. The interpolated profile at the same latitude of the east-west COCORP seismic line is used in magnetic modeling. Across the MGA, the anomaly amplitude is about 600 gammas.

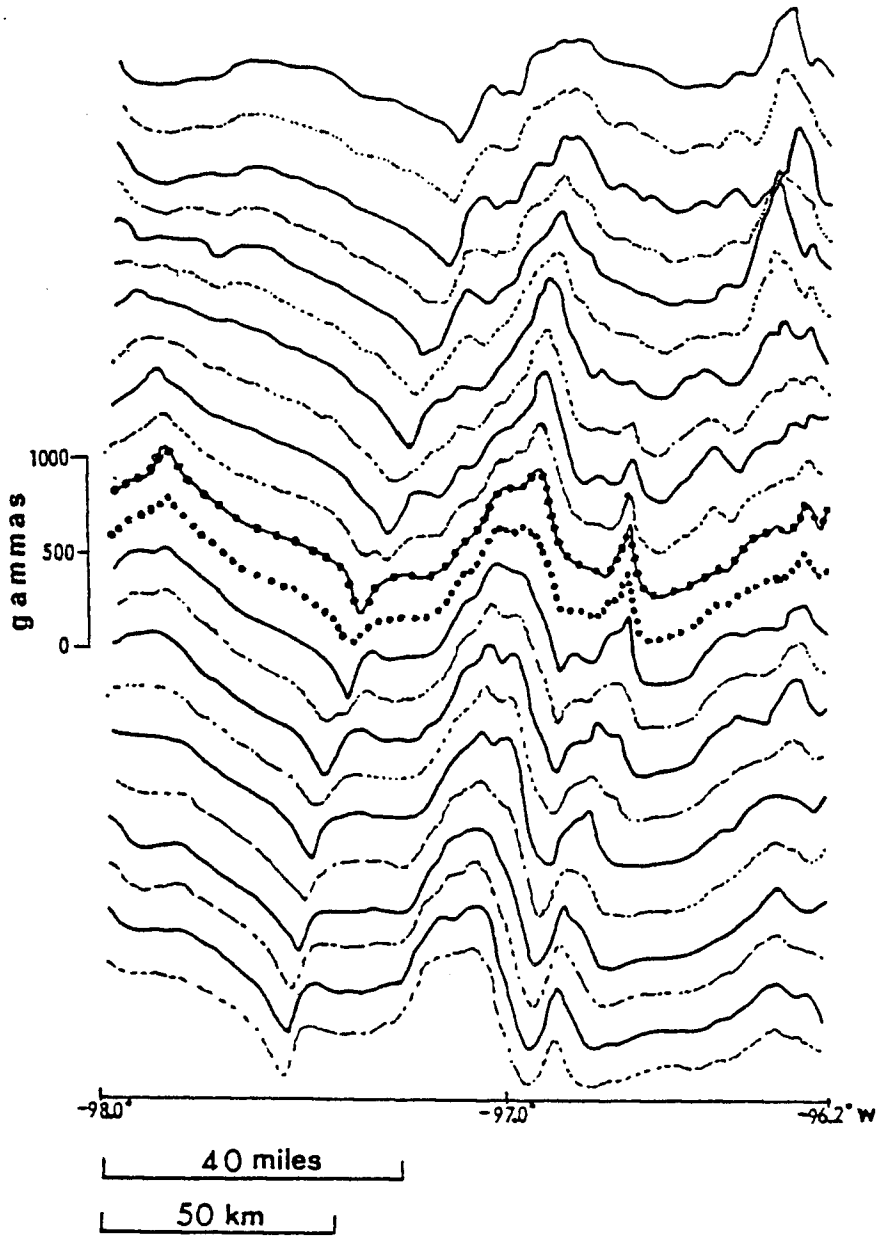

Figure 11. East-west aeromagnetic profiles across the MGA.
North-south spacing between adjacent profiles is 1 mile.
———— Profiles close to measurement paths.
– – – – – – – – Interpolated profiles.
•••••••• Profiles close to COCORP east-west line
(both are 1 mile north and south from
39.625° N latitude).

Modeling Technique

Modeling is the method of deriving a model whose computed effects are in satisfactory agreement with the observations. In potential fields modeling, agreement between observations and computed values does not prove that the model represents the actual situation because of the lack of uniqueness. Therefore, in order to obtain a more reliable and realistic model, other information is needed to constrain and minimize the variety of solutions. In this study the initial model shape is suggested from the interpretation of seismic sections in the same area, combined with available drill hole data. The appropriate gravity and magnetic parameters are assigned to this model. The model is then tested and modified to give its calculated gravity and magnetic values that best fit the observed gravity and magnetic data.

Calculations in gravity and magnetic modeling are based on the gravity and magnetic formulae for a prism-shaped body given by Goodacre (1973) and Bhattacharyya (1964), respectively. The mathematical formulae and computing iterations for one prism are given in Appendix I. In this study, the model shape is approximated by adding many small prisms. The gravity and magnetic values are computed for each prism at the observation

point. Results from all prisms are then added and compared with the observed data at the observation point. Computation is then done for the next observation point and so on, along the selected profile.

Gravity modeling is based on calculation of the vertical component of the gravity field at the point of observation due to the density contrast of the rock body. The density contrast used here is the lateral change in density which would give rise to the gravity anomaly. For example, in an area where density is increasing with depth without lateral changes in density, the corresponding gravity anomaly will be constant.

Magnetic modeling is based on the calculation of the total-intensity magnetic field at the observation point due to net magnetization contrast of the rock body and the effect of the earth's inclined ambient magnetic field. According to the concept of magnetic dipoles, the rock body is assumed to have a continuous distribution of dipoles resulting in a net magnetization vector. The magnetic field due to the net magnetization of the dipoles is calculated along the earth's field direction at the observation point. The calculation is more complicated than for gravity because the magnetic fields are both attractive and repulsive. Magnetization

is the fundamental parameter in magnetic modeling as density is in gravity modeling. However, magnetization is a vector quantity, whereas density is a scalar one.

Usually, magnetization is induced by the earth's magnetic field where the dipoles of magnetic material line up with the earth's magnetic field. The degree to which the rock is magnetized by induction is determined by its magnetic susceptibility k_i defined as

$$\bar{J}_i = k_i \bar{H} \quad ,$$

where $\bar{J}_i$ is the induced magnetization vector and $\bar{H}$ is the earth's magnetic field vector.

In cases where only induction by the earth's magnetic field is assumed, the magnetic susceptibility contrast is the only magnetization parameter required in magnetic modeling. The term "contrast" used here is lateral as in the case of density contrast. Figure 12 illustrates simple cases of the residual magnetic anomalies due to rock bodies of induced magnetization at different latitudes. The long axis of buried magnetic body is perpendicular to the page. At flight elevation, the anomaly is positive, negative, and zero when the field of the magnetized body reinforces, opposes, and is perpendicular to the earth's field, respectively.

However, for the study of Precambrian rocks, the remnant magnetization must be taken into account in

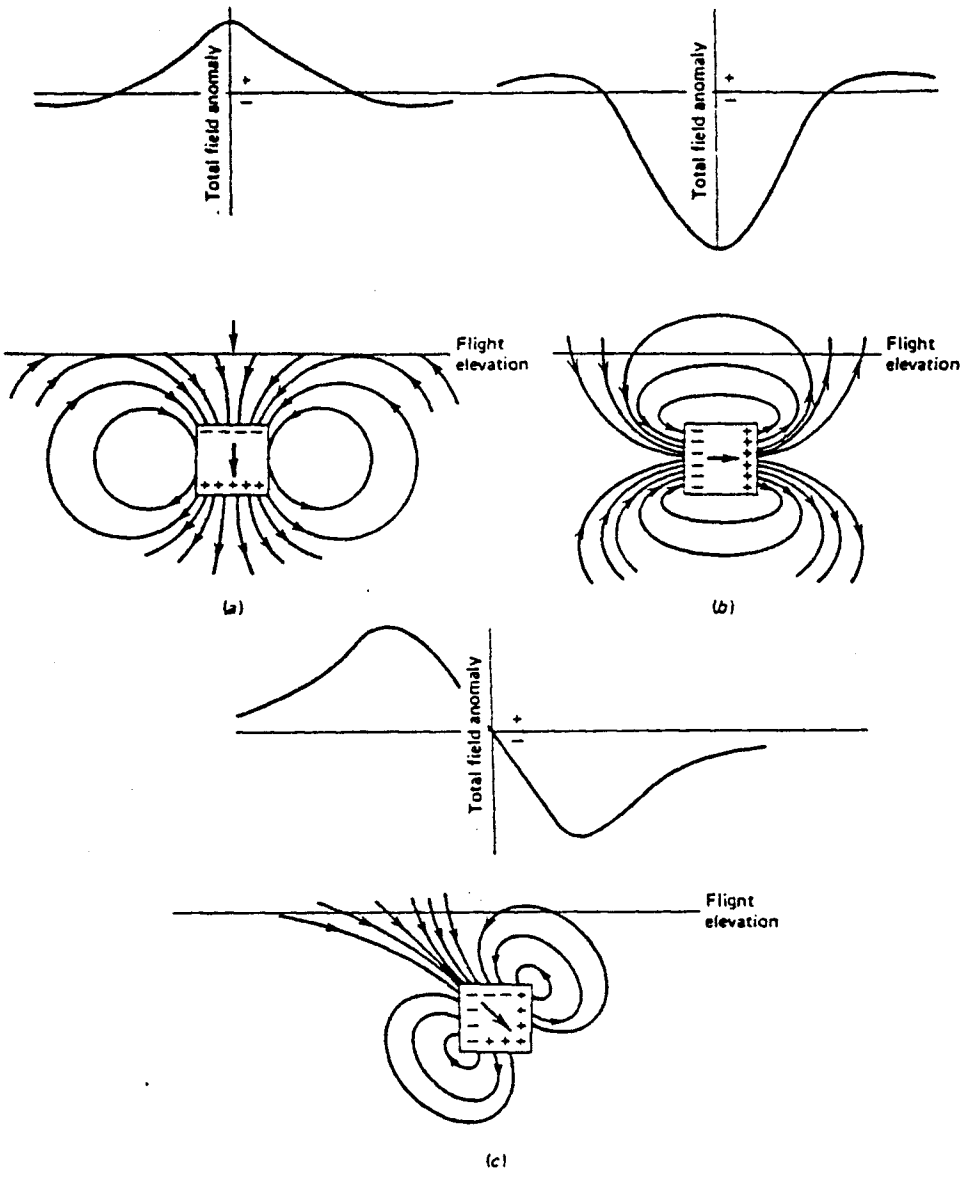

Figure 12. Total magnetic field anomalies (a) at north magnetic pole, (b) at magnetic equator, and (c) at magnetic latitude 45° N. All magnetization is induced. (After Dobrin, 1976).

addition to the induced magnetization. Remnant magnetization is governed by the earth's magnetic field that existed when the rock was formed, provided that no later changes occurred. For igneous rock, the direction of remnant magnetization will be that of the earth's field at the time it cooled down from its initial molten state to a temperature below the Curie point. However, later changes in magnetization direction may occur such as in the case of reheating to its Curie temperature in a different earth's field direction.

Net magnetization due to both induced and remnant magnetizations in a magnetic body can be written as

$$\bar{J}_n = \bar{J}_i + \bar{J}_r ,$$

where $\bar{J}_n$ and $\bar{J}_r$ are net and remnant magnetization vectors, respectively. It can also be written as

$$\bar{J}_n = k_i |\bar{H}| \ (\hat{1}_i + Q \hat{1}_r) ,$$

or

$$\bar{J}_n = k_n |\bar{H}| \ \hat{1}_n ,$$

where $\hat{1}_i$, $\hat{1}_r$ and $\hat{1}_n$ are unit vectors of $\bar{J}_i$, $\bar{J}_r$ and $\bar{J}_n$, respectively, $|\bar{H}|$ is magnitude of the earth's magnetic field, k_n is net magnetic susceptibility, and Q is the ratio of remnant to induced magnetization magnitude.

It is this last relationship that is used in magnetic modeling which allows k_n and $\hat{1}_n$ to be the input parameters in testing of net magnetization $\bar{J}_n$ of the

model.

The ratio k_n/k_i can be derived, based on the law of cosines, as

$$\frac{k_n}{k_i} = \left(1 + 2Q\cos(\hat{1}_i,\hat{1}_r) + Q^2 \right)^{\frac{1}{2}} ,$$

which shows that k_n/k_i depends on the angle $(\hat{1}_i,\hat{1}_r)$ and the Q value. However, for the angle $(\hat{1}_i,\hat{1}_r)$ between $-\frac{\pi}{2}$ and $\frac{\pi}{2}$, k_n/k_i is greater than 1 for any positive Q. k_n/k_i can also be derived as follows:

$$k_n|\bar{H}|\ \hat{1}_n = k_i|\bar{H}|\ (\ \hat{1}_i + Q\hat{1}_r\ )$$

$$k_n\ \hat{1}_n\cdot\hat{1}_n = k_i\ (\ \hat{1}_i + Q\ \hat{1}_r\ )\cdot\hat{1}_n$$

$$\frac{k_n}{k_i} = (\ell+QL)u + (m+QM)v + (n+QN)w$$

where (ℓ,m,n), (L,M,N), and (u,v,w) are direction cosines of $\hat{1}_i$, $\hat{1}_r$, and $\hat{1}_n$, respectively.

Preliminary Modeling - Background

Prior to potential fields modeling, it is appropriate to note some interpretive results from the Bouguer gravity and aeromagnetic maps, along with drill hole data. Effects of the modeling parameters, especially the inclination and declination angles of net magnetization, are also examined. Then, according to the results, the initial model suggested from the COCORP seismic sections is tested and modified to give a best fit to the observed residual gravity and magnetic anomalies.

The interpretation of gravity data is usually straightforward due to the simplicity of the earth's gravity field which is always attractive and vertically downward. Therefore, a positive gravity anomaly generally indicates more dense rocks directly beneath it. A negative gravity anomaly is caused by a negative-density-contrast source; that is, rock that has lower density than that of average crust. The longer wavelength anomaly is usually caused by a deeper source, whereas the sharper anomaly is due to a source at shallower depth.

The Bouguer gravity map (figure 8) shows an average gravity value in the range of -60 to -70 mgal in northeastern Kansas. The northeasterly gravity high of

the MGA ranges from about -60 mgal up to +10 mgal. The flanking lows on both sides are lower than -65 to -70 mgal. Therefore, it can be expected that rocks of positive density contrast lie along the northeasterly trend of the gravity high, and rocks of negative density contrast lie along the trends of gravity lows.

The aeromagnetic map in northeastern Kansas (figure 10) shows average magnetic fields between 1200 and 1400 gammas. The magnetic high of the MGA across the study profile is up to 1650 gammas, and its lows down to about 1000 gammas.

The interpretation of magnetic map is not as straightforward as the gravity because the magnetic fields are both attractive and repulsive. Also, measurements are taken in the earth's field direction that is not vertical.

In the northern hemisphere, a magnetic anomaly high implies a high-magnetic body with its net magnetic field downward. However, the source rock is not necessary located directly beneath the peak of the anomaly high (see for example, figure 12c). Therefore, it can be expected, at least, that the magnetic high of the MGA is due to a high-magnetic body that has its net magnetic field downward. Specific values of inclination and declination are to be tested by modeling based on

available information of magnetization measurements. The lower-than-average anomaly may be due to the extreme depth to magnetic basement, or a source rock with little or no net magnetization, or the edge effect of the high-magnetic body, or the magnetic field reversal at parts of the source rock which results in alternate highs and lows as in case of the mid-oceanic ridge.

Comparison of the aeromagnetic map (figure 10) with the Bouguer gravity map (figure 8) in northeastern Kansas, especially in the MGA area, reveals obvious correlations, even though in detail the magnetic anomaly is more irregular than the gravity. The axes of both gravity and magnetic anomaly highs lie along the same northeasterly trend of about 30° clockwise from north. However, the peak of the magnetic high is slightly shifted from that of the gravity high. Along the east-west COCORP seismic line, the peak of the magnetic high is located at about VP (vibration points) 1650-1750, while the gravity peak is at about VP 1700-1800.

The magnetic anomaly of the MGA has a shorter wavelength than the gravity anomaly. There is a secondary magnetic high (at about VP 1450-1470) that lies parallel to the primary high along the southeastern side of the MGA. Its northeasterly trend, 30° clockwise from the north-south direction, coincides with the

boundary between the gravity high and the eastern gravity low. Thin section studies from Precambrian well cuttings (Bickford, personal communication, 1984) indicate 7 wells of olivine-bearing gabbroic rocks along the trend of this secondary magnetic high.

On the northwestern side of the MGA, the trend of magnetic low (at about VP 2000-2100) also coincides with the boundary between the gravity high and the northwestern gravity low. This trend is approximately 45° clockwise from the north.

Thin section studies also reveal abundant wells of Rice formation in the MGA area, especially on its eastern flank in the study area. Along the COCORP line, the wells are located between VP 1250 and VP 1500 which is in the area of the eastern gravity and magnetic lows of the MGA. However, from VP 1250 eastward to beyond the Nemaha Ridge, well cuttings are dominated by sheared granites that characterize the basement terrane in Kansas.

Ground surface in the area of study is regionally flat, about 400 m above sea level. The Precambrian basement surface revealed by drill data (Cole, 1976) is slightly dipping to the west. The Paleozoic sediments are about 1 km thick, except over the Abilene anticline (about 700 m) and the Nemaha Ridge (about 200 m). The

gravitational effect of the Paleozoic section in the MGA zone is negligible due to its small and approximately constant thickness. The strata are also considered to be non-magnetic because of the negligible magnetite content in sedimentary rocks compared to mafic igneous rocks.

Preliminary Modeling - Modeling Parameters

In gravity and magnetic modeling, the modeling parameters are size, location, orientation, density, and net magnetization of the model. Given the same model shape, a deeper body results in a longer wavelength and lower amplitude anomaly. Increasing density and susceptibility contrasts result in higher amplitudes of the gravity and magnetic anomalies, respectively.

We now consider the effect of different net magnetization directions. Net magnetization direction is expressed in terms of inclination and declination angles. Inclination angle (I) is measured positively downward, and negatively upward, relative to the horizontal plane. Declination angle (D) is measured positively clockwise, and negatively counterclockwise, on the horizontal plane from the north direction. Figures 13 and 14 show the effect of varied inclinations at D = 0° and -40°, respectively. And figure 15 shows the effect of varied declinations at I = 50°. The orientation of the profile and the magnetized body is the similar to that of the MGA and the east-west study profile. The north direction is inwardly perpendicular to the page. The long axis of prismatic body is 30° clockwise from the north. The earth's field is 68° of inclination and 7° of declination.

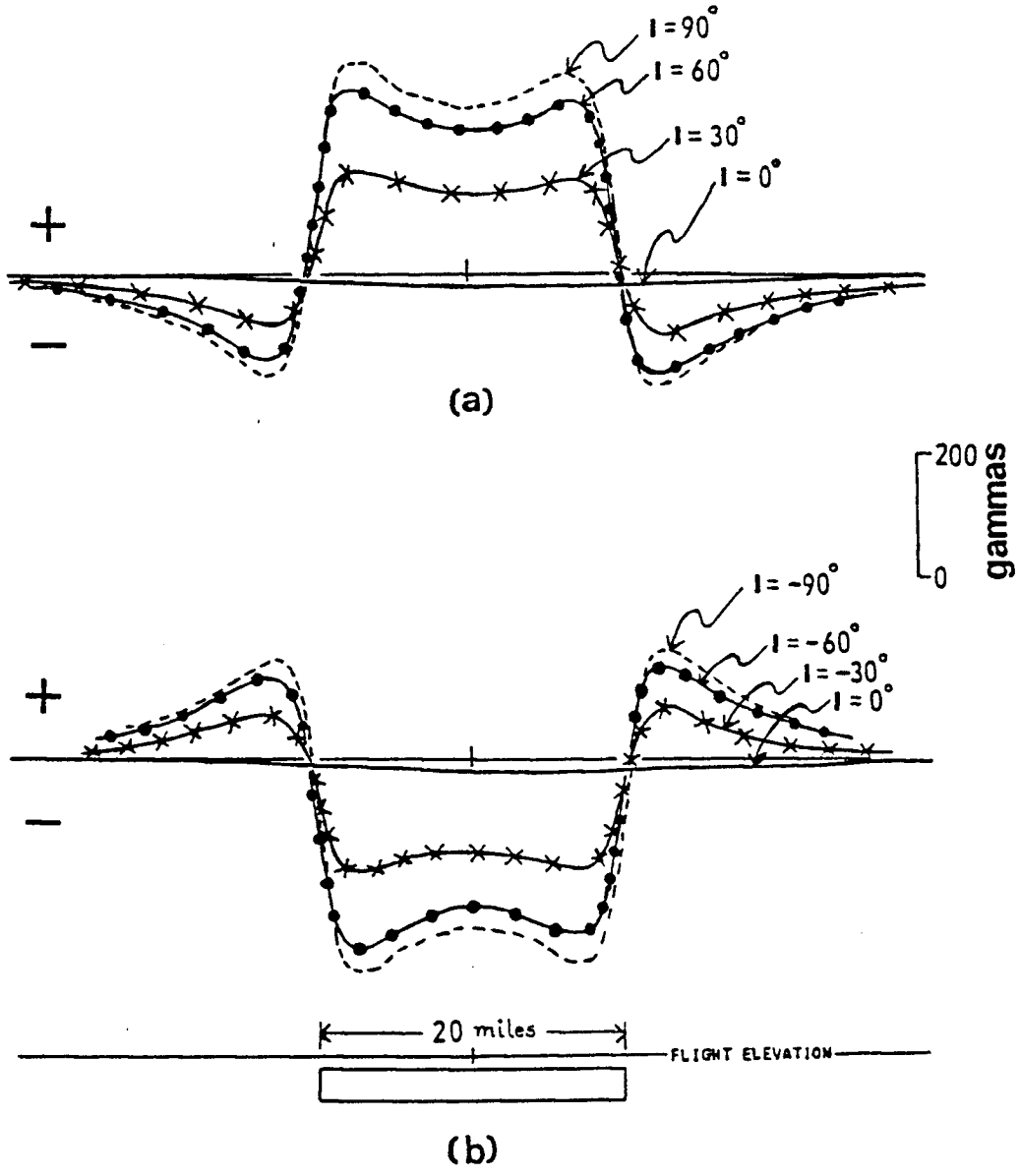

Figure 13. Total magnetic field anomalies in Kansas for varied inclinations at zero declination. Net susceptibility contrast = 0.004 cgs.
(a) Positive or downward inclinations.
(b) Negative or upward inclinations.

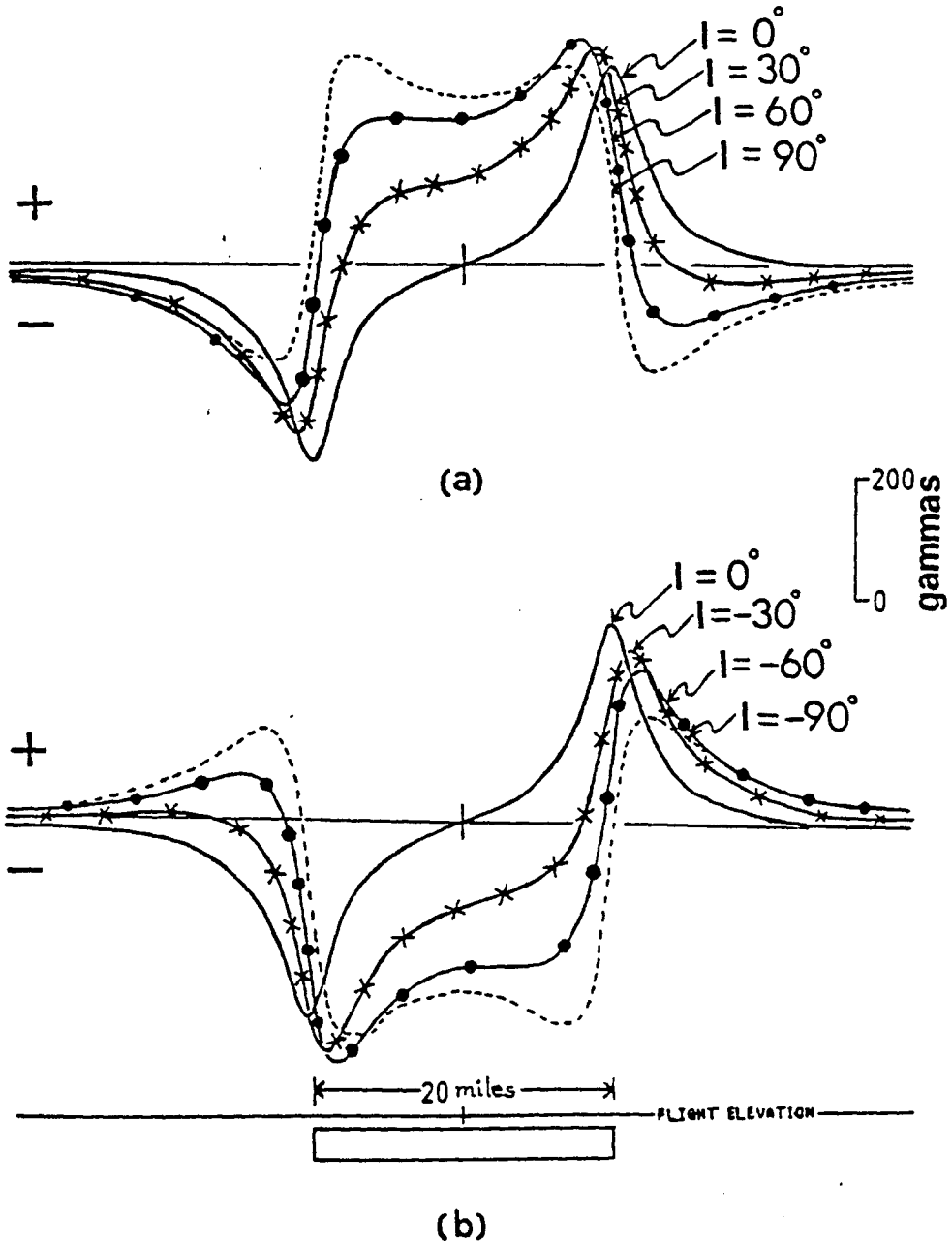

Figure 14. Total magnetic field anomalies in Kansas for varied inclinations at -40° declination. Net susceptibility contrast = 0.004 cgs.
(a) Positive or downward inclinations.
(b) Negative or upward inclinations.

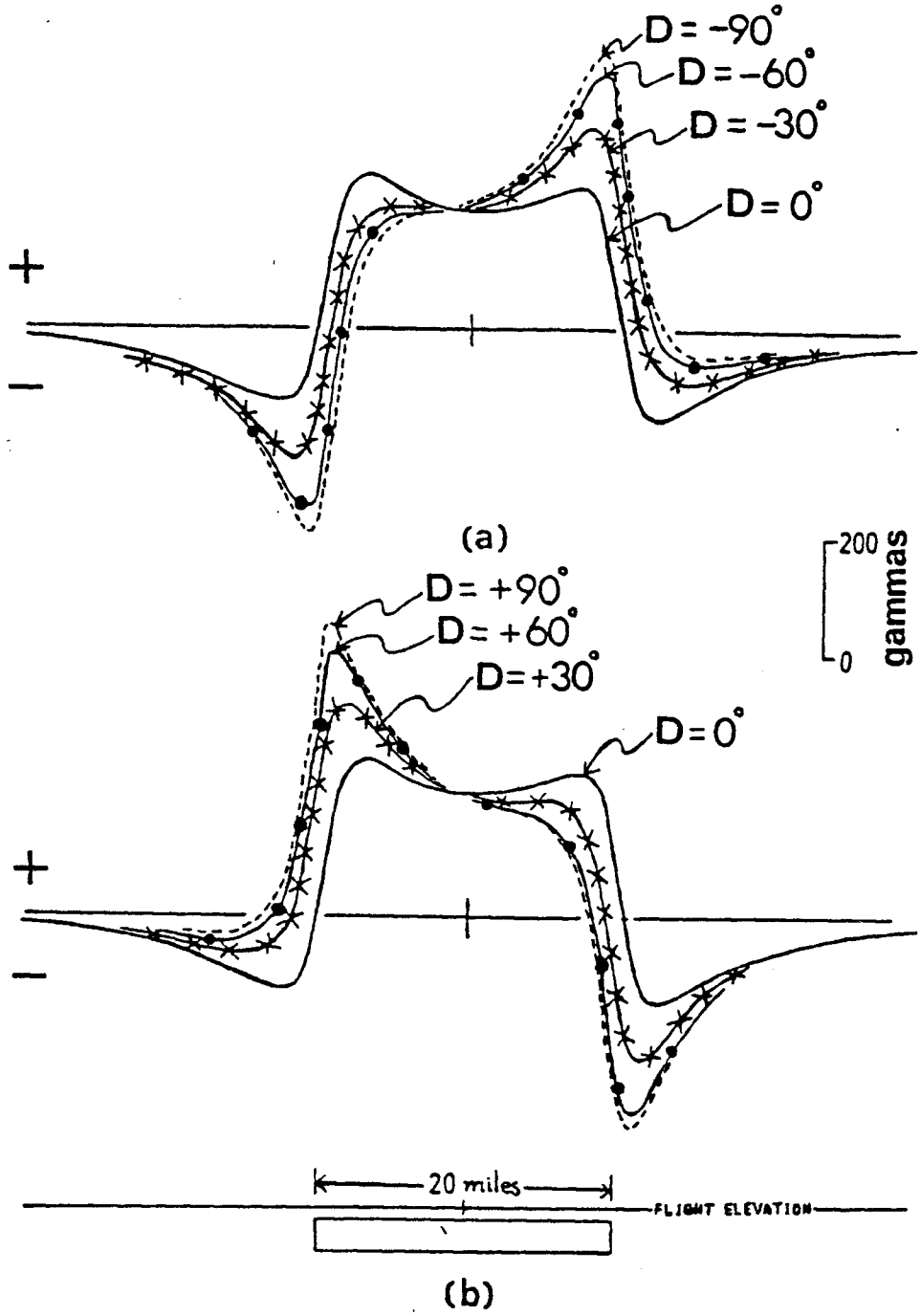

Figure 15. Total magnetic field anomalies in Kansas for varied declinations at +50° inclination. Net susceptibility contrast = 0.004 cgs.
(a) Fourth quadrant declinations.
(b) First quadrant declinations.

Varied inclinations result in amplitude changes of the anomaly. This is obvious in figure 13 where the anomaly amplitude increases toward $I \approx 90^{\circ}$ and decreases toward $I \approx 0^{\circ}$. In figure 14, similar changes in amplitude can be seen, even though the anomaly at the egdes of the body looks irregular due to a nonzero declination.

Varied declinations (figure 15) affect the anomaly at the edges of magnetized body. At the center of the body the anomaly remains at the same level, in contrast to figures 13 and 14.

In short, inclination affects anomaly amplitude, especially at the central part of the body. Declination affects anomaly shape at and near the edge of the body.

Preliminary Modeling - Result

In this section, both gravity and magnetic modeling are used to test the model suggested from the COCORP seismic section. The profile of study is the 160 km (100 mile) long east-west line along the COCORP seismic profile across the MGA, at 39.625° N latitude. For gravity modeling, the acceptable range of density contrast for mafic rocks compared with granitic rocks is 0.2-0.3 gm/cm^3, where the density of granite is normally 2.6-2.7 gm/cm^3 and that of mafic rocks is 2.9-3.0 gm/cm^3 (see for example, Telford and others, 1976, p. 26; White, 1966, p. E5).

The regional trend of gravity is subtracted from the observed Bouguer gravity anomaly, resulting in the observed residual anomaly to be used in modeling. The linear regional trend, along the study profile, has a base level of -60 to -70 mgal, and is slightly dipping to the east with a gradient of .07 to .12 mgal/km (which may be due to some other sources of different density on both sides beyond the MGA, or by crustal thinning to the west, or both). The eastern boundary of Rice formation (at about VP 1250 - 1300) on the east end of the study profile is revealed by drill cuttings (Bickford and others, 1979). It can be used to define the regional trend by allowing the negative anomaly to extend

eastward not far beyond the limit of the Rice formation.

Mafic rocks such as basalts and gabbro have much higher magnetizations than silicic rocks such as granite and rhyolite (see for example, Telford and others, 1976, p. 21; Yarger, 1983, pp. 20,23), so that, in terms of magnetization contrast, the granitic crust is assumed to be nonmagnetic compared to mafic rocks. The induced magnetic susceptibility contrast Δk_i of mafic rocks is in the range of 0.001 to 0.003 cgs. The net susceptibility contrast Δk_n will be higher than Δk_i for $|\theta| < \frac{\pi}{2}$, where θ is an angle between induced and remnant vectors (p. 31).

The magnetization of Keweenawan mafic rocks near Duluth, Minnesota (Jahren, 1965), corresponds to an apparent paleopole position around latitude 30° to 34° N and longitude 175° to 180° W. Based on this Keweenawan pole position, the earth's magnetic field in Kansas during Keweenawan time pointed west-northwest and downward, with average inclination of 40° and declination of 290°. This calculation also assumes that since Keweenawan time, Kansas and Minnesota have not drifted apart from one another but maintained the same relative positions as parts of the North American tectonic plate.

Therefore, based on the assumption above, the direction of remnant magnetization in Kansas during the

Keweenawan period would be around 40° inclination and 290° declination. The resultant vector of net magnetization, to be used in magnetic modeling, will then be approximately in the fourth quadrant, that is, in between directions of remnant and induced magnetizations depending on the Q value. Thus, the net inclination should be from 40° downward to 68° and the net declination from -70° clockwise to 7°.

A flat magnetic regional trend of 1250 gammas was subtracted from the observed magnetic anomaly, resulting in the residual magnetic anomaly used in the magnetic modeling.

Finally, with the acceptable range of input parameters mentioned above, the asymmetric basin filled with interbedded basalts and clastic rocks, interpreted from COCORP seismic section across the MGA (Serpa and others, 1984) (figure 7), is tested and modified. The east-west cross section of the model and anomalies are shown in figure 16. The long axis (about 80 miles) of the model is rotated 30° clockwise from the north direction which is inwardly perpendicular to the page, and the east-west profile is across the center of the model. The datum elevation is at sea level for gravity modeling, and at the flight elevation of 760 m above sea level for magnetic modeling. The parameters that yield

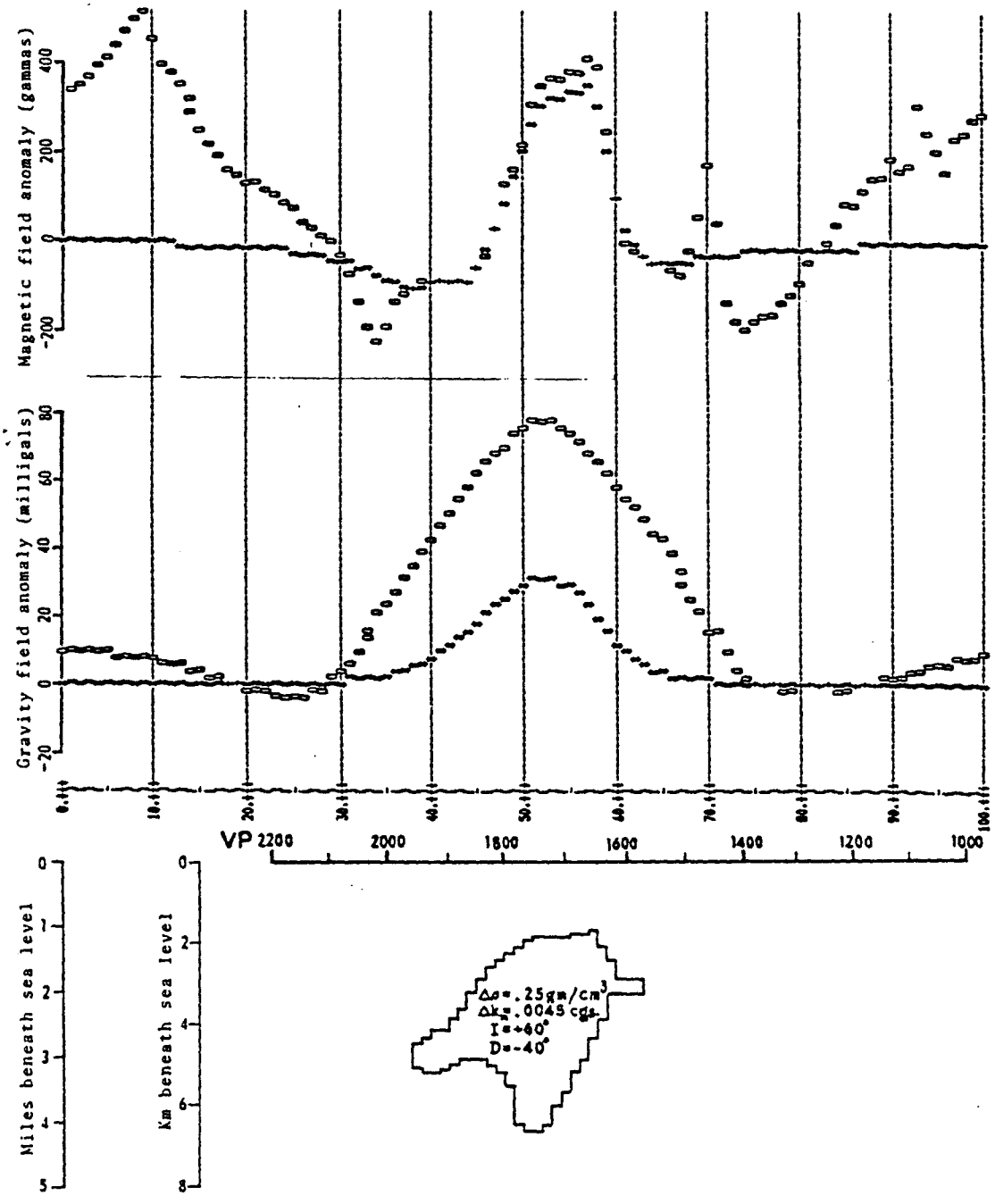

Figure 16. Gravity and magnetic modeling of an asymmetric basin filled with interbedded basaltic and clastic rocks, interpreted from COCORP seismic section. The horizontal scale is in miles eastward from 98° W longitude.

-------- = Modeled anomaly, oooooooo = Measured anomaly.

best agreement between the simultaneously modeled and measured profiles are: $\Delta\rho = 0.25$ gm/cm^3, $\Delta k_n = 0.0045$ cgs., $I = 60^\circ$, and $D = -40^\circ$.

It is obvious that the gravity anomaly due to the basaltic rift basin is about half the amplitude of the MGA and also has a shorter wavelength. An unacceptably high density contrast of at least 0.5 gm/cm^3 is required to match the amplitude of the MGA but not the wavelength, as mentioned by Serpa (personal communication, 1984).

The magnetic effect of the basaltic rift basin is interesting. Its wavelength fits that of the primary magnetic high of the MGA, and nearly does for its amplitude. The favorable direction of net magnetization is in the fourth quadrant, at $I = 60^\circ$ and $D = -40^\circ$.

The net magnetization direction at $I = 60^\circ$ and $D = -40^\circ$ infers that remnant magnetization is important in addition to induced magnetization. According to the induced direction of $I_i = +68^\circ$ and $D_i = +7^\circ$, by using the remnant direction of $I_r \approx +40^\circ$ and $D_r \approx -70^\circ$ with $Q \approx 1$, the net magnetization direction can be calculated to be in agreement with the one derived from modeling ($I_n = +60^\circ$, $D_n = -40^\circ$). The calculated ratio $\Delta k_n/\Delta k_i$ is about 2. Therefore, the high value of Δk_n, which is

required to match the magnetic anomaly (Δk_n = 0.0045cgs. in this modeling), is acceptable.

It should be noted also that the east end of the basaltic rift basin is at about VP 1560. Therefore, the seismic data seem not to infer the source of the secondary magnetic high (at VP 1460) to be due to a magnetic reversal (as in case of the mid-oceanic ridge), or to be due to the thin edge effect of a large magnetic body at shallow depth (as in case of modeling by Yarger (1980), shown in figure 6), because in such cases the east end of the basaltic rift basin is required to extend eastwardly to at least at VP 1460.

Reprocessing part of the seismic data in this area, which is discussed in the following sections, was done in order to bring out the possible interpretation of this secondary magnetic high. After that, the derived model was tested again through potential field modeling. Discussion of the deeper mafic source suggested from gravity modeling (Serpa and others, 1984) and the arkosic sedimentary basins on both sides of the MGA is also postponed to that section.

SEISMIC REFLECTIONS

Data Acquisition Parameters

The Consortium for Continental Reflection Profiling (COCORP) survey has acquired deep seismic reflection data in northeastern Kansas during 1979-1981. The east-west profile is 194 km long across the Nemaha Ridge and the MGA. Preliminary results, using standard COCORP data processing (Schilt and others, 1979), were reported by Brown and others (1983), and Serpa and others (1984).

The objective of the survey is to detect and image deep geologic structures in the continental crust through the seismic reflection technique. By generating seismic waves at ground surface, the attempt is to digitally record waves reflected back from interfaces of rock layers that have different acoustic properties. The acoustic properties of rocks, ie. seismic wave velocity and rock density (whose product is acoustic impedance), are related primarily to the mineralogic composition and rock type.

The energy source used to generate seismic waves is Vibroseis (trade mark of Continental Oil Company) employing five large truck-mounted vibrators that emit oscillatory energy of continuously increasing frequencies from 8 to 32 Hz during the 32-second sweep.

Subsequent data processing, by cross-correlation of the received signal with the source signal itself, reduce the data so that the source appears to have been an impulse.

The emitted signal from the Vibroseis source has a much lower amplitude than that from an explosive source, which makes it desirable in populated areas. In addition, it has high penetration due to the duration over many seconds of the source, and the low frequencies of the emitted signal which decay slower with distance than higher frequencies (see for example, Telford and others, 1976, pp. 240-242). The penetrated distances of energy to the deep crust, and possibly to sub-Moho discontinuity depths in northeastern Kansas (about 35-40 km), are indicated in seismic sections interpreted by Brown and others (1983).

A 96 channel digital recording system is used, with a low-pass filter of 31.25 Hz and sample rate of 8 milliseconds. At each receiver group 24 geophones, each with natural frequency of 7.5 Hz, are connected in series along the profile. The configuration of geophone grouping between VP 1360 - 2234 is shown in figure 17b, where the spacing of adjacent geophones is 4.3 m. Addition of signals detected by these geophones within the group, when the source is in line with the geophone

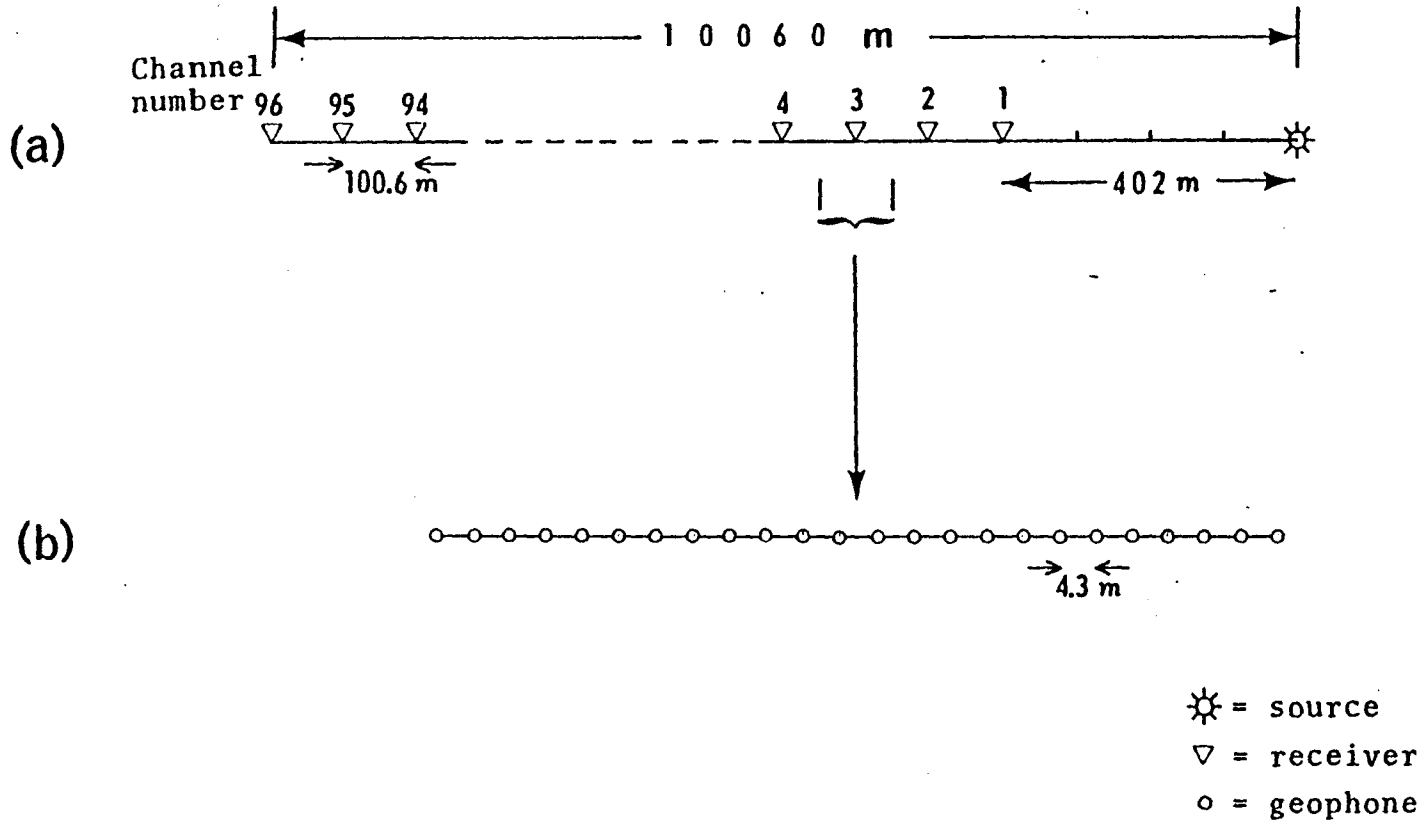

Figure 17. (a) Pattern of an 'end on' spread with 96 channels. There are 24 geophones connected in series per channel.

(b) Configuration of geophones grouping.

array, results in some cancellation of unwanted ground roll due to low-velocity and low-frequency surface or near-surface waves (see for example, Dobrin, 1976, pp. 100-107). Random or incoherent noise, due to energy scattering from near-surface irregularities, will also be attenuated within the geophone group.

The geometric arrangement of source and receivers (figure 17a) is an "end on" spread type, where the source is located at one end of the spread, 402 m (1320 ft) from the first receiver. The distance between adjacent receivers is 100.6 m (330 ft). The spread covers 6.1875 miles, approximately 10 km.

The common-depth-point (CDP) method (Mayne, 1962) is used. The entire spread and the vibration trucks are shifted 100.6 m along the profile after each source vibration. The advantage is that each common subsurface reflection point is sampled up to 48 times with different source-to-receiver distances (figure 18). One CDP-gather has up to 48 seismic traces or 48 fold. These traces are processed so that they would appear to have a zero source-to-receiver distance, and are summed to form a single stacked trace.

The final seismic section consists of orderly CDP-stacked traces. It looks very much like a cross section of the earth underneath the seismic line, where the

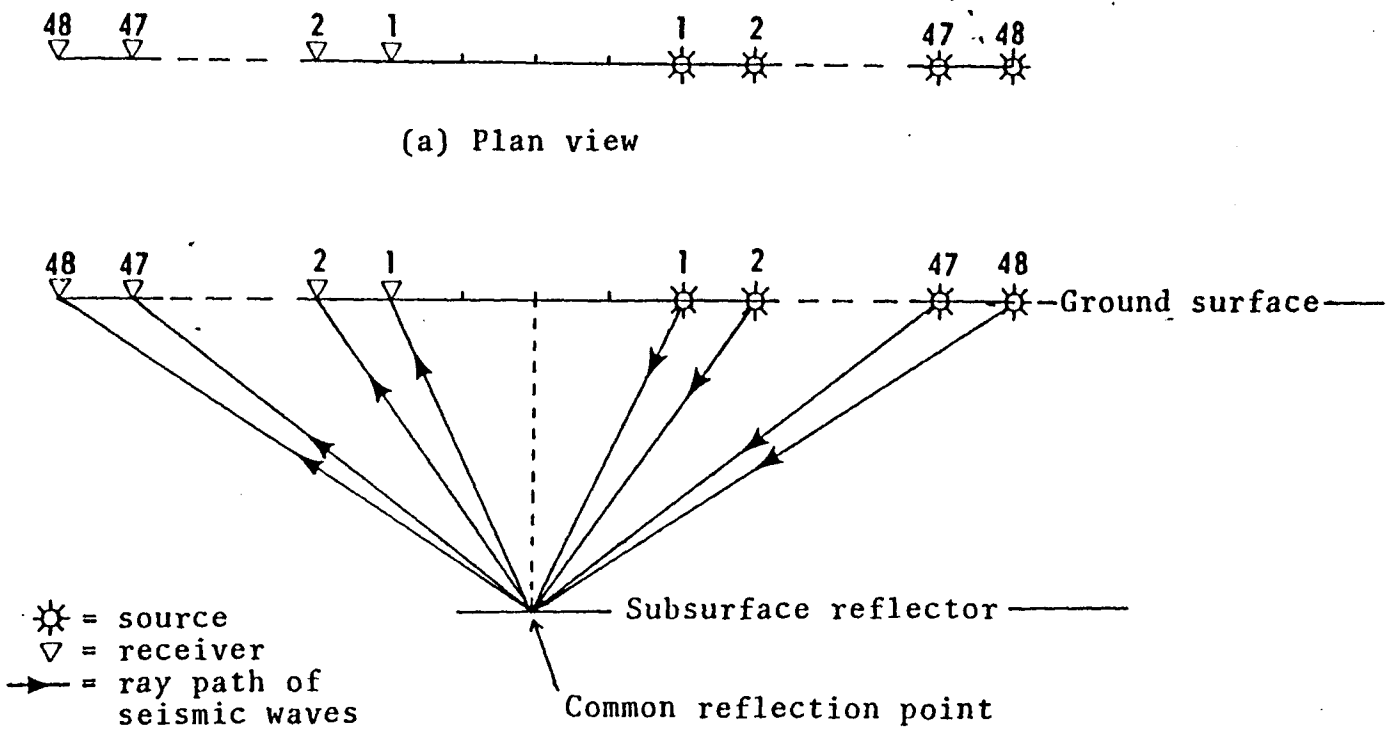

Figure 18. Common-depth-point (CDP) method for 96 channels. One CDP-gather has up to 48 seismic traces or 48 fold.
(a) Plan view of a CDP-gather.
(b) Cross sectional view of a CDP-gather.

vertical scale is two-way travel time. Information of geologic structure and rock type can be interpreted mainly from reflection time and sometimes from amplitude and frequency information shown in the seismic record sections.

Reprocessing

In this study, reprocessing part of the COCORP seismic data (VP 1400 - 1500) was done along the profile on the east side of the MGA, across the Abilene anticline. There are two primary reasons for this. First, the secondary magnetic high in this area, which marks the southeastern flank of the MGA (figure 10) indicates the presence of highly magnetic rocks in the upper crust. The steep horizontal gradient of the anomaly suggests that these rocks could be fairly shallow. The magnetic properties of the rocks are not related directly to their acoustic properties; however, seismic sections of improved quality in this area might reveal clues for the possible interpretation of this secondary magnetic high.

Second, there are procedures to improve quality of the seismic sections. In the vicinity of the secondary magnetic high, the seismic profile is shifted 1.6 km (1 mile) southward at VP 1454. As a result, there are data recorded when the source is in the north line and receivers are in the south line. The CDP-profile for such data lies midway between and parallel to both the north and the south lines (figure 19). Each CDP-gather consists of different source-to-receiver directions (figure 19), instead of one direction as in the usual

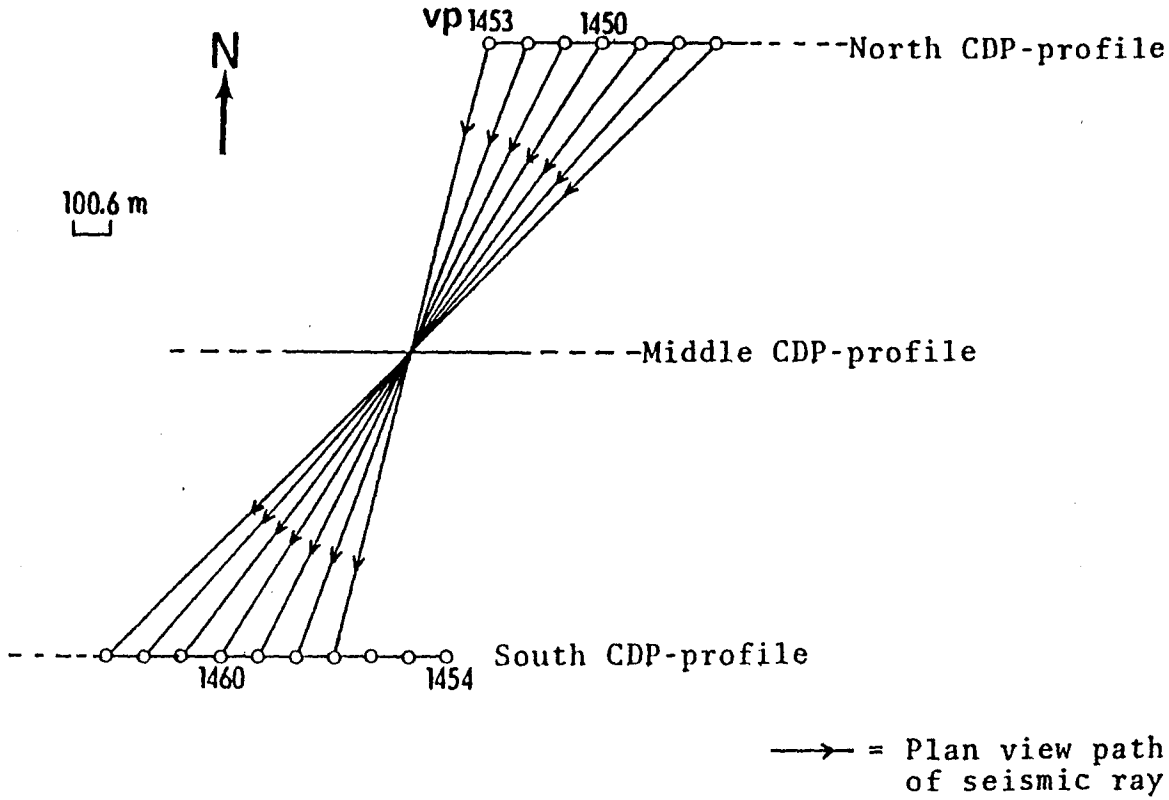

Figure 19. Plan view showing the north, middle, and south CDP-profiles, where the east-west seismic line is shifted southward 1 mile at vibration point (VP) 1454.

case (figure 18a). Therefore these data were reprocessed separately from the north and the south CDP-profiles.

Also, due to such field arrangement, the unwanted ground roll and other noise are not properly cancelled within the geophone group, especially for the near receivers in the south line when the source is near in the north line. The seismic section across the area, shown in figure 20, displays the severe disturbance of ground roll noise between VP 1440 - 1480 and times 0.6 - 1.8 seconds. Therefore, reprocessing was done in order to carefully minimize this ground roll problem.

COCORP seismic data between VP 1400 and VP 1500 for the upper 3 seconds of two-way travel time were reprocessed at the Kansas Geological Survey, using the SPEX (Seismic Processing EXecutive, Sytech Corporation) seismic processing system.

After entering information from field notes (eg. ground surface elevation and location of vibration points, pattern of source and receivers, etc.), the seismic data were sorted into CDP-gathers in 3 separated CDP-profiles: the north, the middle, and the south CDP-profiles. The middle CDP-profile consists of data recorded when the source is on the north line and receivers on the south line.

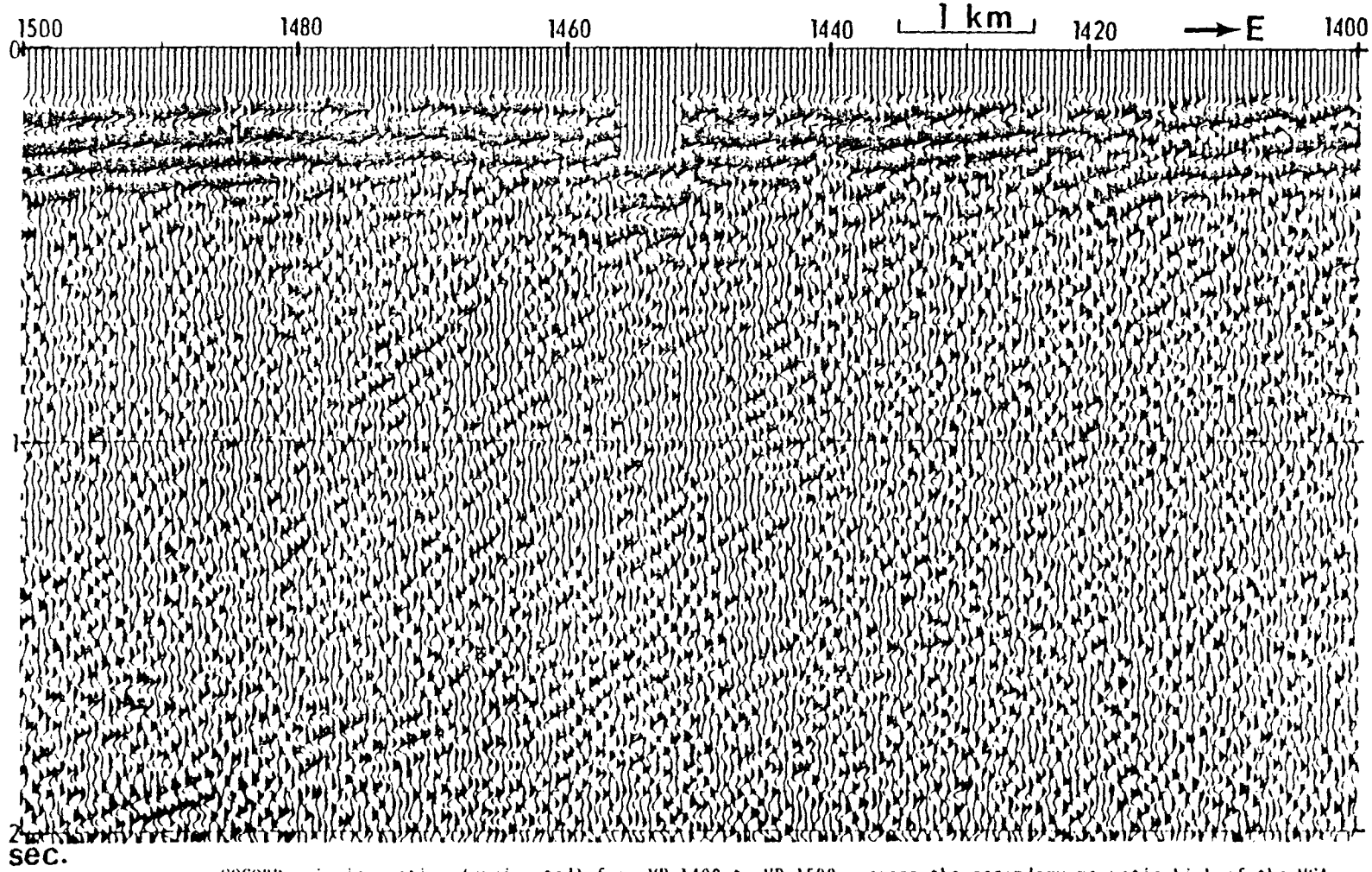

Figure 20. COCORP seismic section (unmigrated) from VP 1400 to VP 1500, across the secondary magnetic high of the MCA. The datum elevation is 150 m above the sea level. The section shows the ground roll noise between VP 1440 to VP 1480 and two-way travel times of 0.6 to 1.8 seconds.

The reprocessing sequence, starting from the correlated data, included: CDP sorting, datum static correction, trace equalization, first arrivals and ground roll muting, stacking velocity analysis, normal move out correction, CDP stacking, and band-pass filtering. The resulting reprocessing parameters are in Appendix II.

Careful reprocessing is emphasized on the middle CDP-profile since it is severely disturbed by ground roll noise. Also, it is the profile of interest where the peak of secondary magnatic high approximately bisects the center of the profile (at VP 1462). Samples of CDP-gathers within this middle CDP-profile are shown in figures 21 and 22 for CDP 2904 to CDP 2908 (VP 1452 to VP 1454) and CDP 2916 to CDP 2920 (VP 1458 to VP 1460), respectively. Reprocessing, with careful muting (or zeroing) of ground roll next to the first arrival zone, significantly improves the result. The first arrivals and ground roll muting zone is shown in figure 21 for CDP 2908 (VP 1454). The final CDP-stacked section is shown in figure 23. The dipping strong reflector, indicated by arrows in the figure, appears at a time of about 1.8 s at VP 1450 and 2.1 s at VP 1480.

It is interesting to note the disappearance of the same reflector between VP 1455 and VP 1465 (at time 1.8

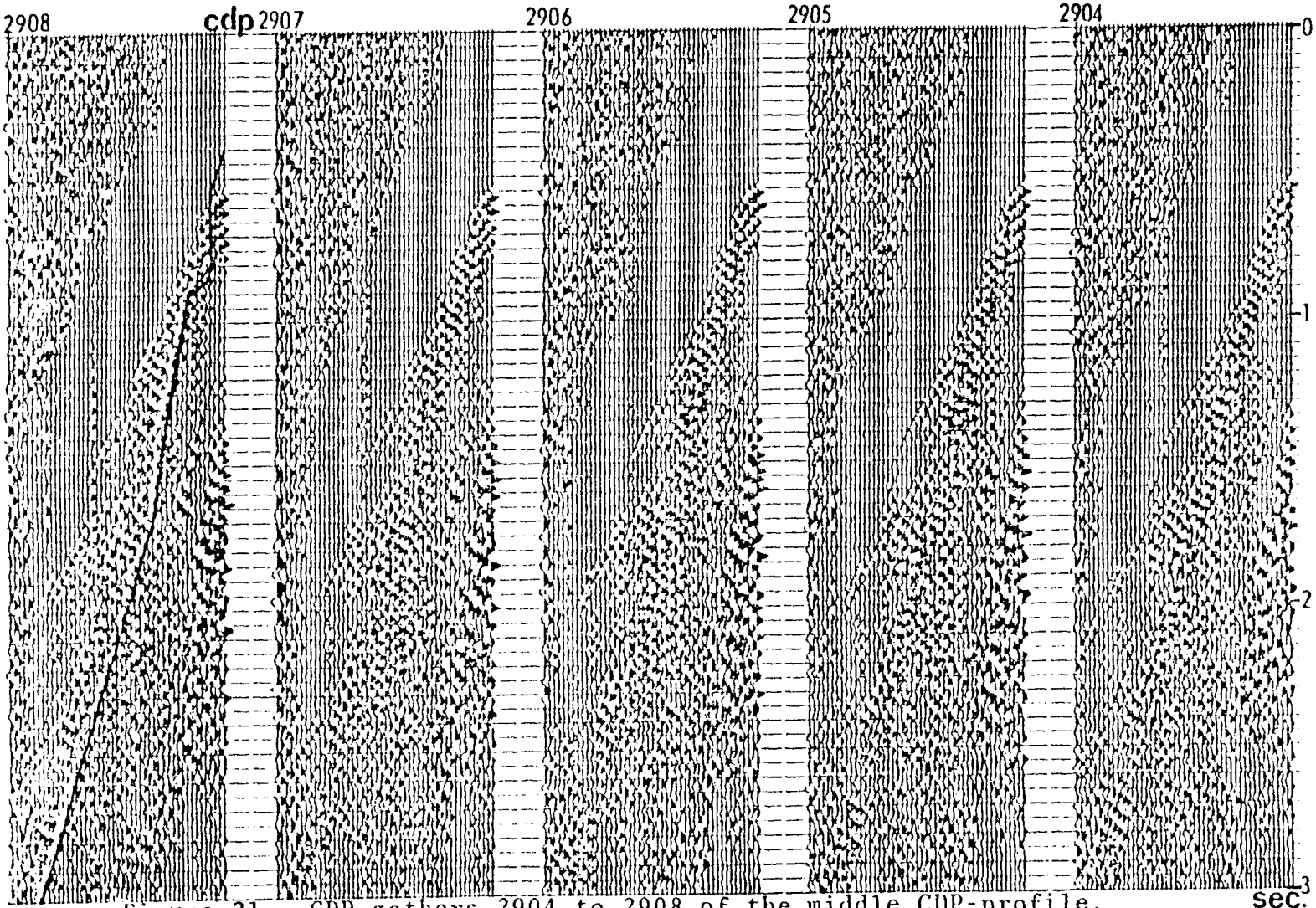

Figure 21. CDP-gathers 2904 to 2908 of the middle CDP-profile.

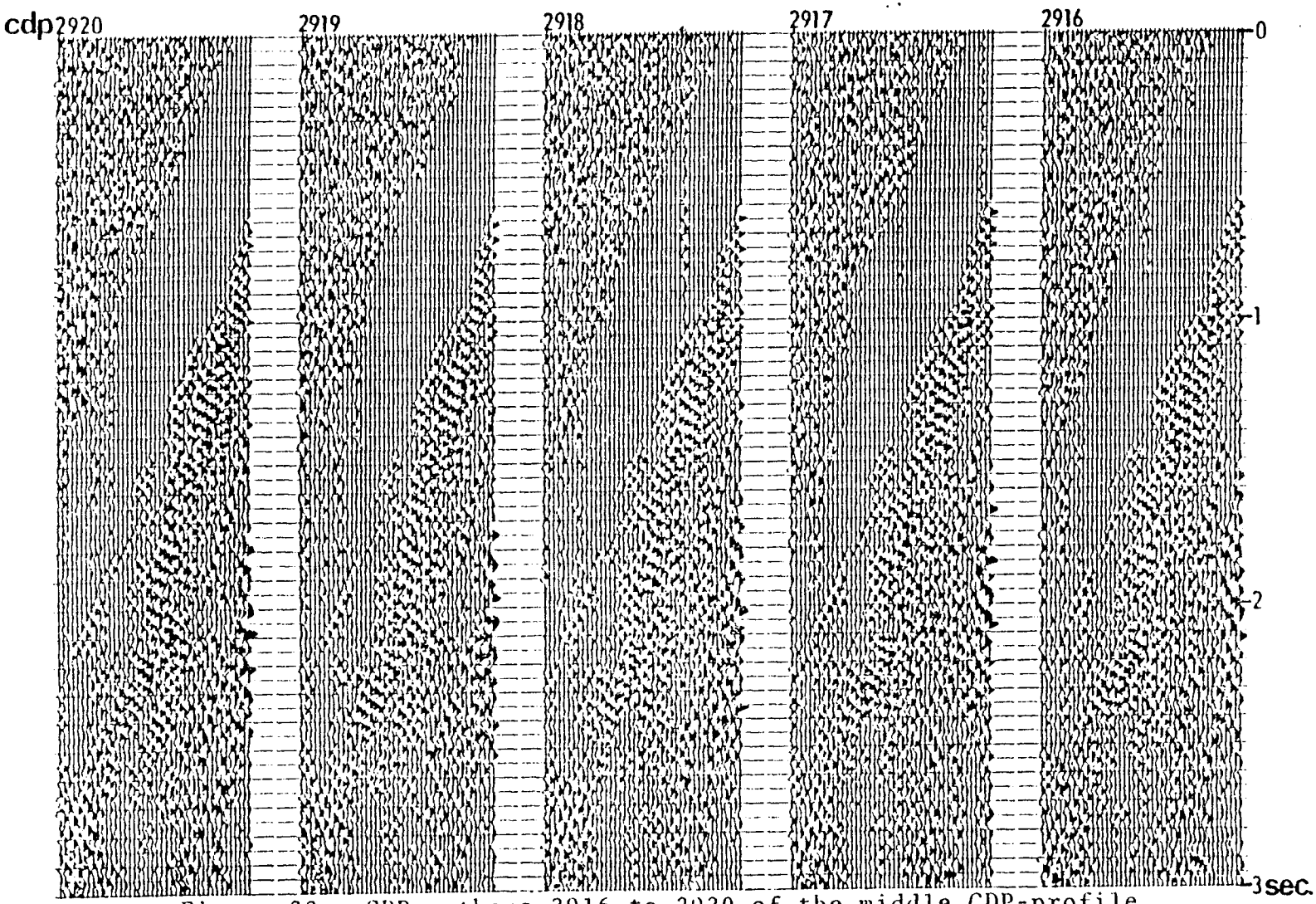

Figure 22. CDP-gathers 2916 to 2920 of the middle CDP-profile.

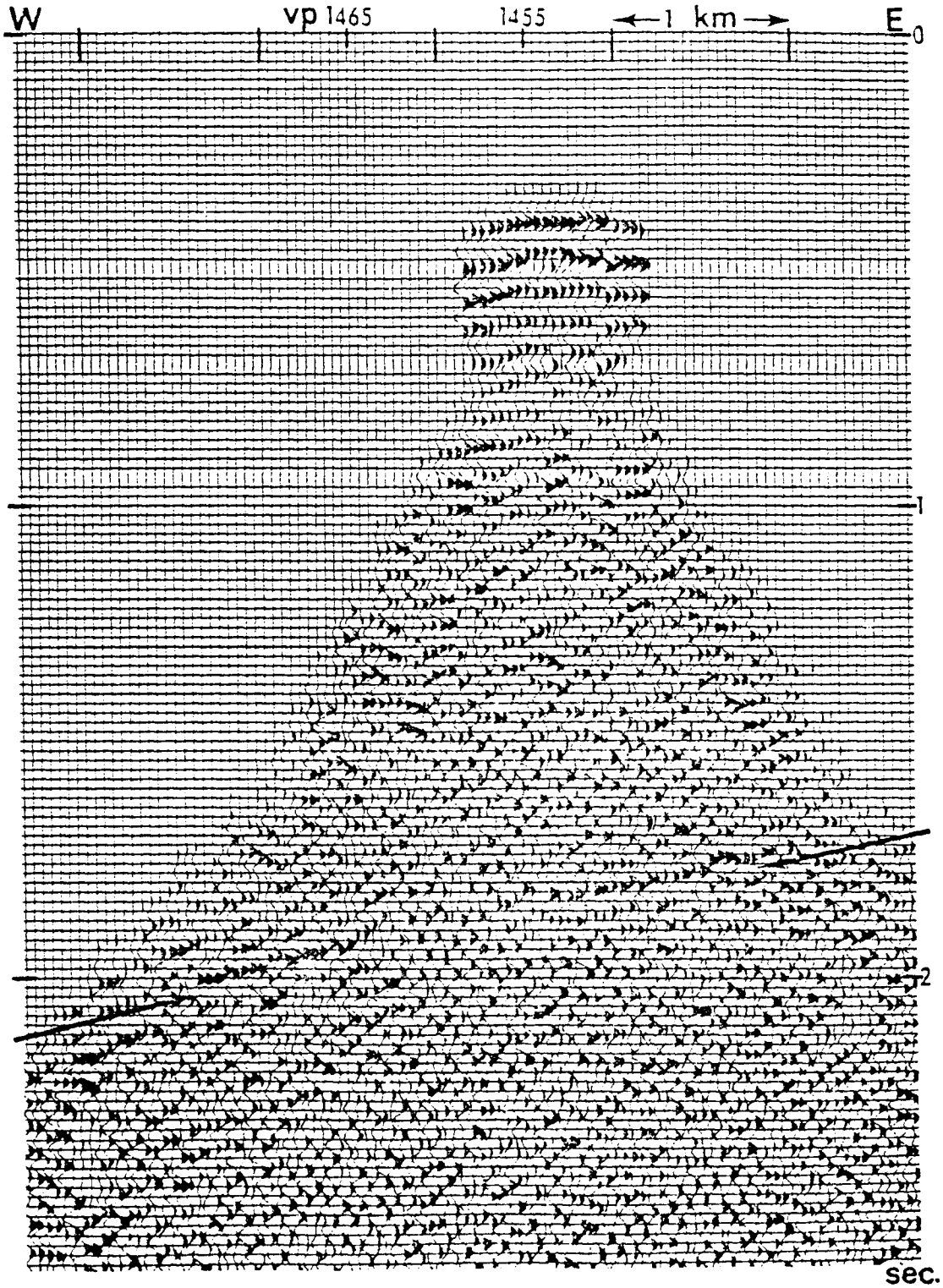

Figure 23. Seismic section of the middle CDP-profile.

- 2.0 s). At first, it seems that the seismic character in this range is dominated by high-amplitude noise like that appearing in CDP-gathers 2916 to 2920 (VP 1458 to VP 1460) shown in figure 22. There the noise is evident between about time 1.5 to 2.5 s for the 12 near-traces. However, this same character also appears in other CDP-gathers such as CDP 2904 to 2908 (VP 1452 to VP 1454) shown in figure 21. But such noise is not dominant in these CDPs in the final stacked section of figure 23 (CDP number is twice VP number). Instead, a strong reflector appears at these CDPs. Therefore, it is likely that the disappearance of a strong reflector between VP 1455 and VP 1465 (at time 1.8 - 2.0 s) is not due to the disturbance of high-amplitude noise.

Note that the amount of fold for each CDP-stacked trace in the middle CDP-profile reduces toward both ends of the profile. The central part of the profile (VP 1447 - 1462) has a higher fold number, including both near and far source-to-receiver distances within each CDP-gather. Toward both ends of the profile, each CDP-gather has only far traces. It is interesting to equalize the fold amount along the profile by neglecting near traces that contain high-amplitude noise (eg. first 12 near-traces in each CDP-gather shown in figure 21 and 22). The CDP-gathers will be equalized both in number

of fold and source-to-receiver distances so that the resulting stacked traces in the section are statistically balanced. In doing this, shallow information is lost. The result is shown in figure 24 for 6-fold data, where only the 25th to 36th channels (total is 12 channels) for each vibration are used. The discontinuity of reflector at time 1.8 to 2.0 s between VP 1455 and VP 1465 is also affirmed in this section.

In addition, the automatic residual static correction is applied to the middle CDP-profile to remove residual static after datum static and normal move out corrections. The same reflector is used as a center of the 600-millisecond window. Because of the dipping of the reflector, only 3 CDPs are used to sum at a time to form the pilot trace for cross-correlation purpose. The maximum allowable static correction is 20 ms. The result is shown in figure 25. The zone of discontinuity (time 1.8 - 2.0 s between VP 1455 and VP 1465) shown in this figure indicates that it is not due to the static problem.

Therefore, the discontinuity of the reflector is more likely to be due to geologic structure rather than processing artifacts. The layered reflection of strong impedance contrast could be disconnected by mafic intrusion of a later event which, due to its high

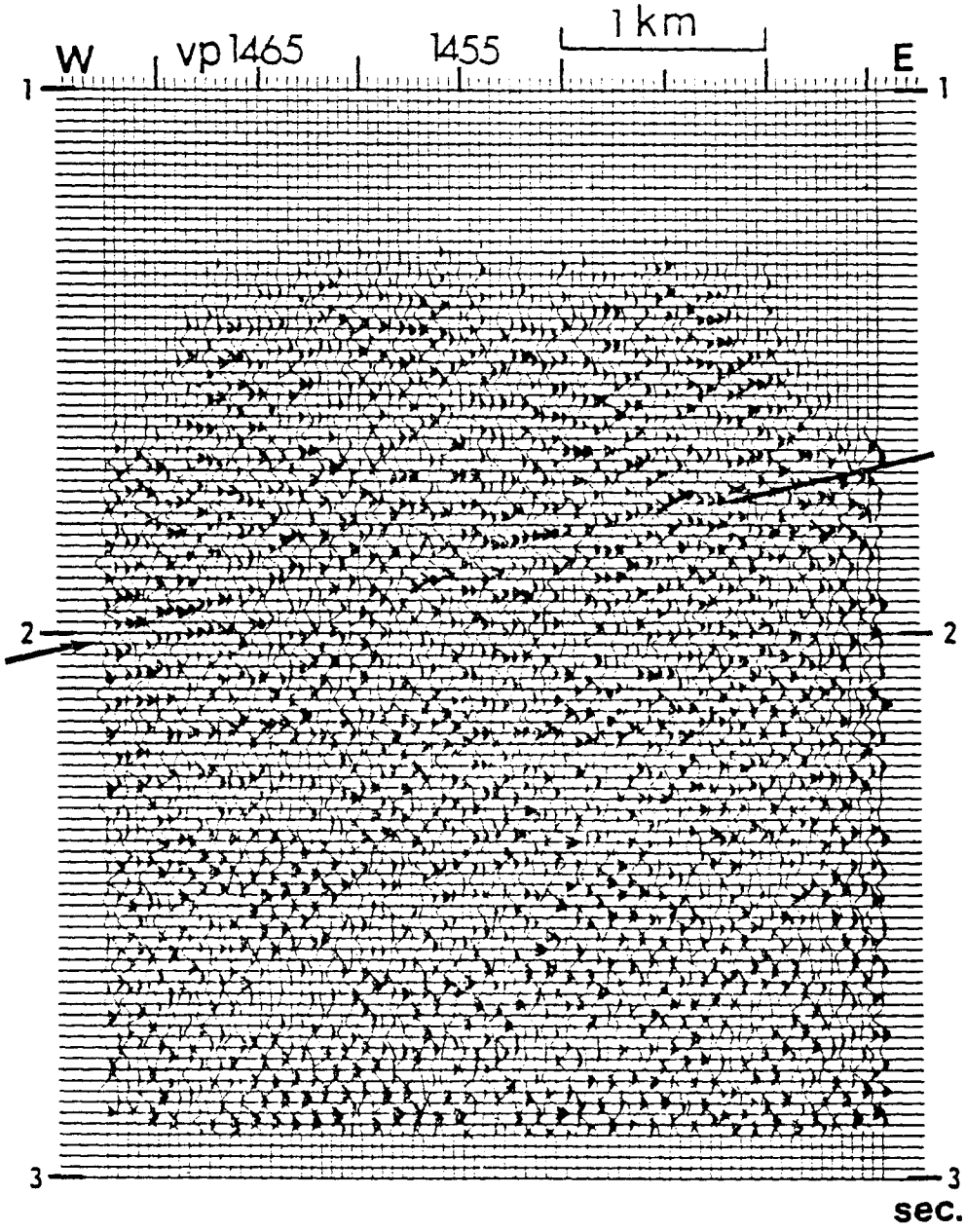

Fig. 24. 6-fold data of the middle-CDP-profile, using the 25th to 36th channels for each vibration.

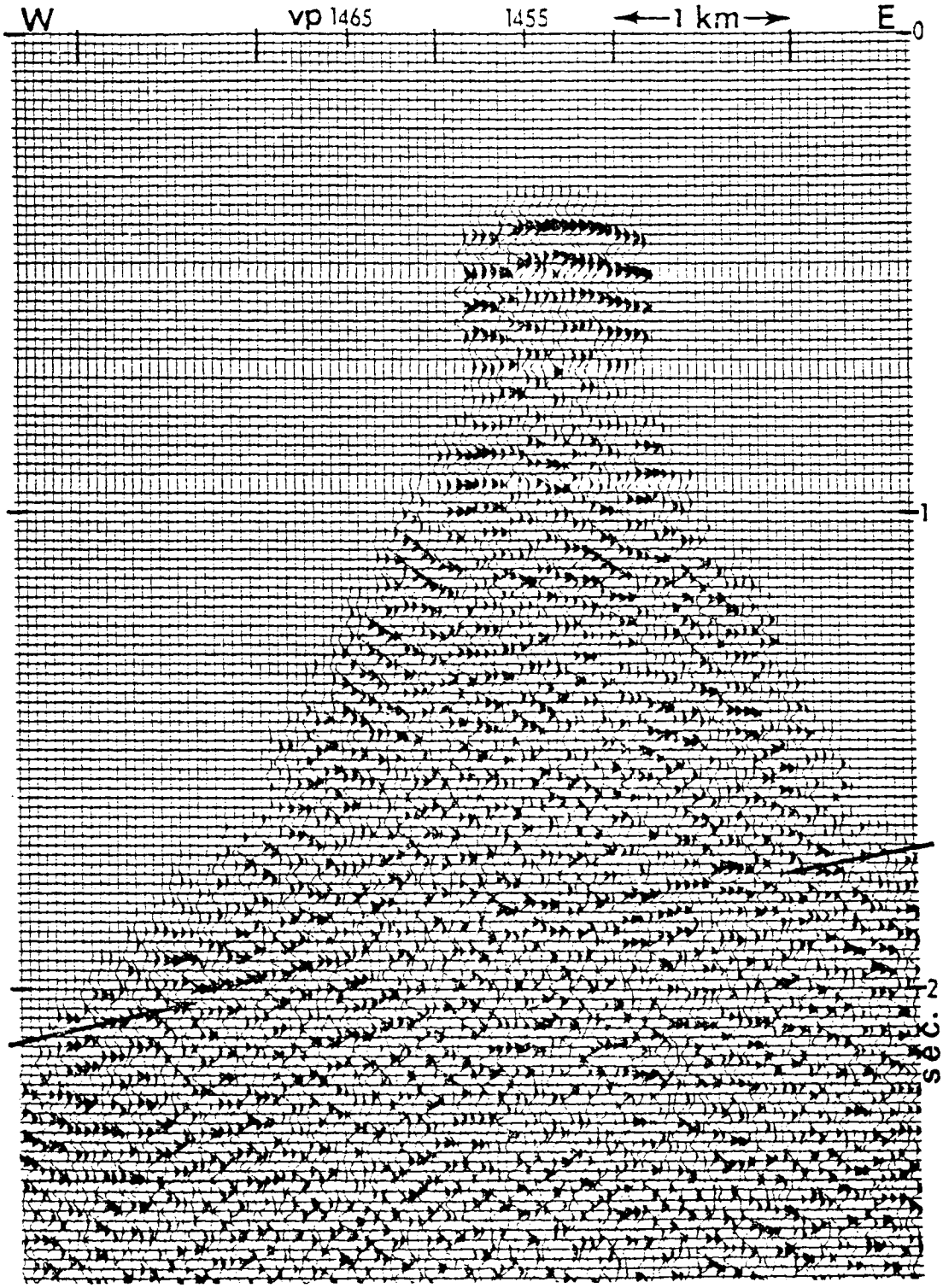

Fig. 25. The middle CDP-profile with automatic residual statics correction.

magnetite content and shallow depth, produces a magnetic high above it. According to the seismic section, the intrusion is located between VP 1455 and VP 1465, so that its center (VP 1460) is at the same location of the secondary magnetic high. Seven wells of olivine-bearing gabbro revealed from thin section studies (Bickford, personal communication, 1984) are indicated along the trend of the secondary magnetic high and may be related to the interpreted mafic intrusion.

Final sections of the north and south CDP-profiles are shown in figures 26 and 27, respectively. The sections do not show significant improvement compared with figure 20. Note the small number of fold at the west and the east ends of the north and the south CDP-profiles, respectively. The reflector appears at time 1.85 s at the west end of the north CDP-profile. It also appears in the south CDP-profile from VP 1500 at time 2.2 s, with gentle slope, up to VP 1470 at time 1.9 s. Even though the west end of the profile has small fold number, however, the fading of the reflector may be due to intrusion as interpreted from the middle CDP-profile.

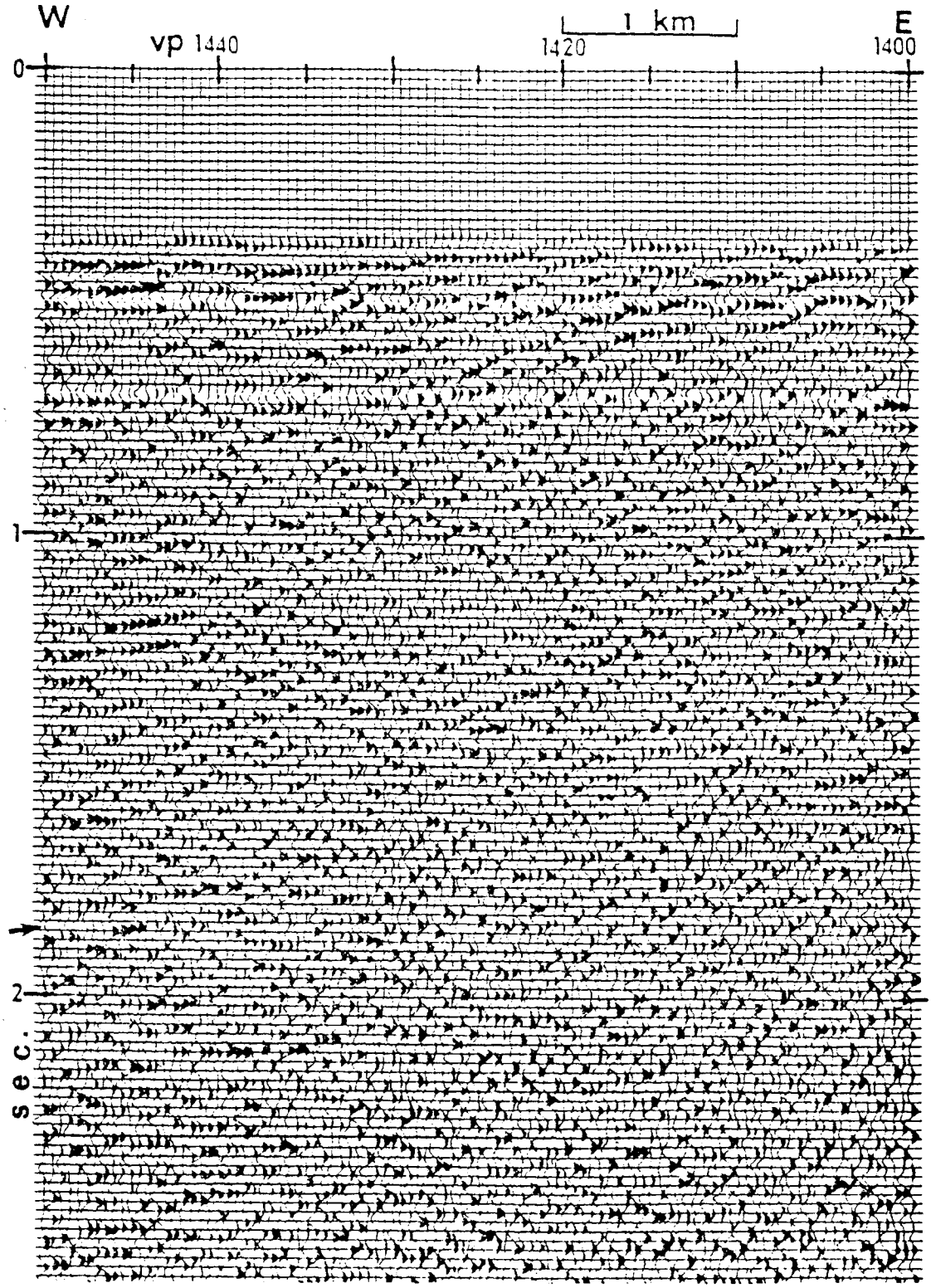

Figure 26. Seismic section of the north CDP-profile.

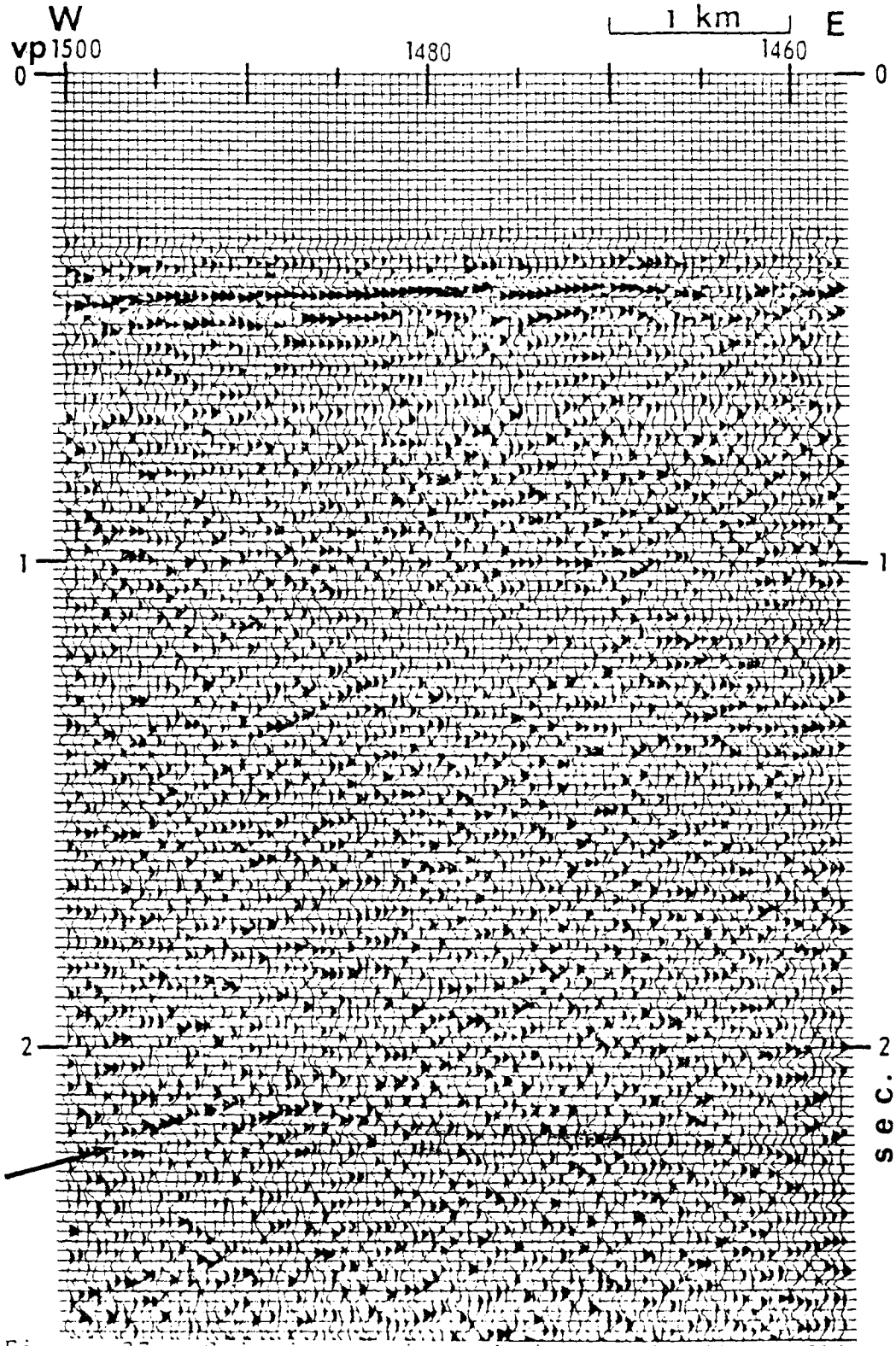

Figure 27. Seismic section of the south CDP-profile.

REMODELING

The discontinuity of layered reflectors shown in seismic sections (figures 23, 24, and 25) suggests a possible mafic intrusion beneath the secondary magnetic high of the MGA. The mafic intrusive body located between VP 1455 and 1465 has an east-west width of about 1 km. The zone of discontinuity shown in seismic sections beneath VP 1460 at two-way time 1.8 - 2.0 s is equivalent to about 5 km depth, assuming an average crustal velocity of 6 km/s (see for example, Brown and others (1983), p. 27). Therefore, the intrusive body is at least 5 km deep. The top of the body is not indicated in the seismic sections, but according to the anomaly sharpness of the secondary magnetic high and mafic wells encountered in the related area, it could be at shallow depth, possibly near the Precambrian surface.

The mafic intrusive body is modeled by a highly magnetic sheet-like shape, with its long axis 30° clockwise from the north. The result of this addition to the original basaltic rift basin model of figure 16 is shown in figure 28. The magnetization direction of the mafic intrusive body is in the first quadrant (I = +70°, D = +40°). The difference in magnetization direction from the basaltic rift basin infers that the intrusive event occurred at a different ambient earth's

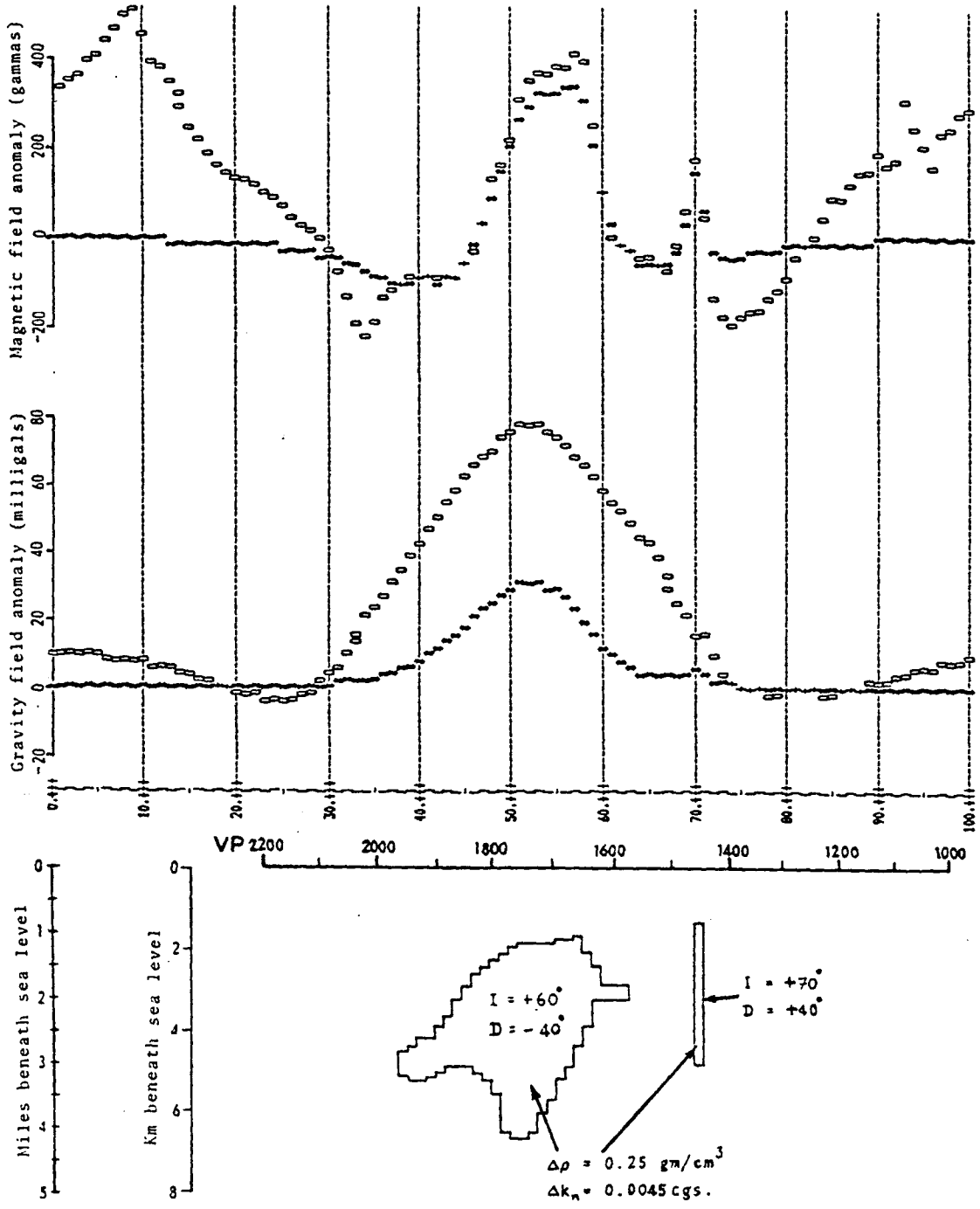

Figure 28. Gravity and magnetic modeling of basaltic rift basin model (of fig. 16) plus an isolated mafic intrusive model (at VP 1460) interpreted from reprocessing of seismic data.
The horizontal scale is in miles eastward from 98° W longitude.
---------- = Modeled anomaly, oooooooo = Measured anomaly.

field. That is, it is a different age.

Based on the study of paleopoles of North America since Precambrian time by Irving (1979) using the minimum polar path, the ambient magnetic earth's field in eastern Kansas can be calculated and is shown in figure 29 for normal polarity (Yarger, personal communication, 1984). Due to paleoinclinations shown in the figure, the drifting path of Kansas, as part of the North American tectonic plate, was from the southern hemisphere at 1.20 b.y. ago and passed the equator at 1.05 b.y. ago into the northern hemisphere. The Keweenawan ambient field, measured by Jahren (1965) to be downward ($I=+40^{\circ}, D=-70^{\circ}$), requires the reversal of polarity in figure 29 between at least 1.15 to 1.10 b.y. old. It is interesting that at the later time of 1.0 b.y. ago, for normal polarity, the ambient earth's field is in the first quadrant ($I=+50^{\circ}$ to $+70^{\circ}$ and $D=+60^{\circ}$ to $+80^{\circ}$). If this is used as remnant magnetization direction of the shallow mafic intrusive model (at VP 1460), in addition to induced magnetization ($I=+68^{\circ}$, $D=+7^{\circ}$), the net magnetization direction will be in agreement with the resulting parameters ($I=+70^{\circ}$, $D=+40^{\circ}$) required by magnetic modeling. Therefore, based on paleopoles study, it is possible that mafic intrusion at VP 1460 is younger than the basaltic rift basin.

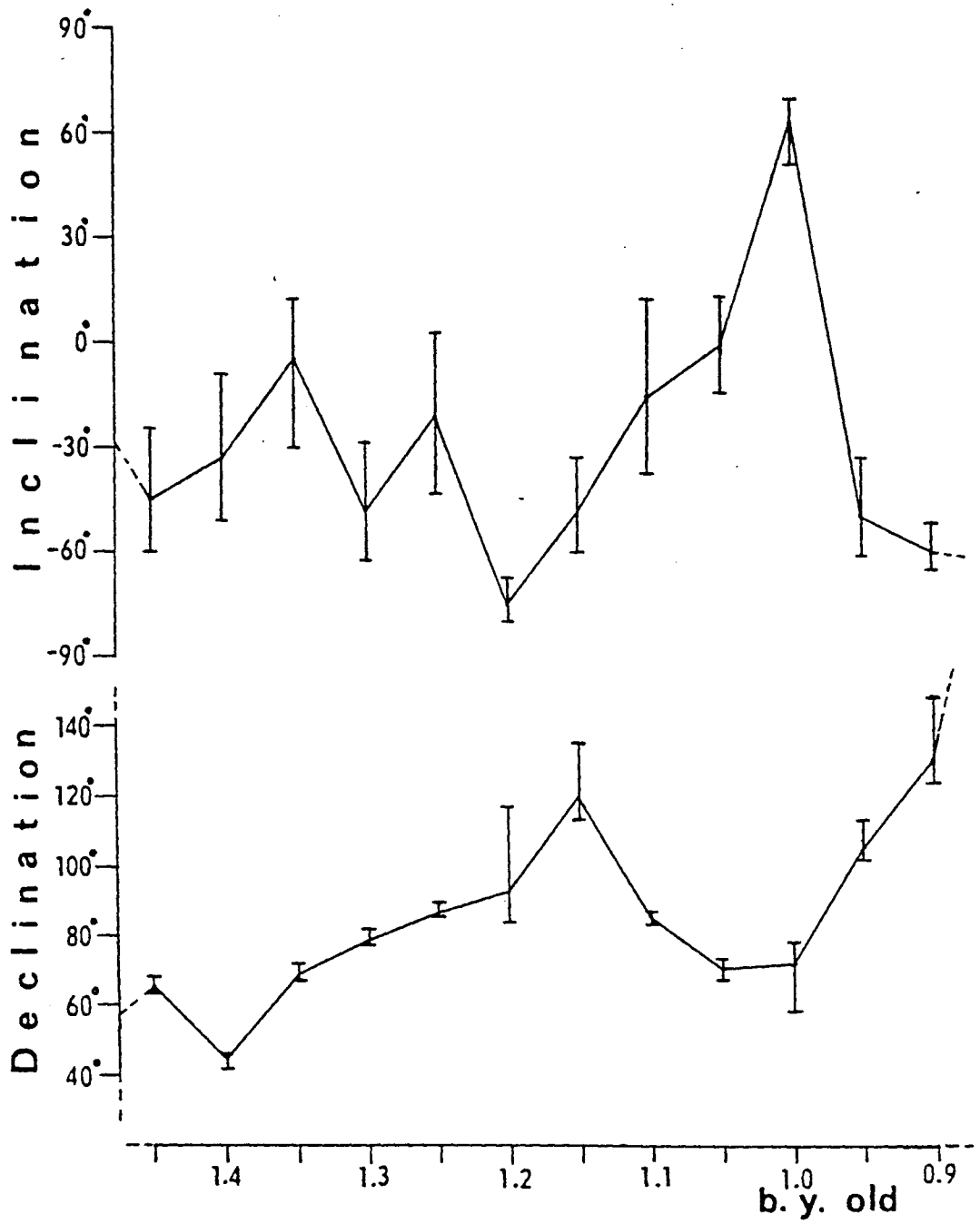

Fig. 29. Paleoinclination (above) and paleodeclination (below) in northeastern Kansas for normal polarity, based on paleopoles study of North America by Irving (1979), where vertical bar represents the possible range of inclination or declination angle according to the width of apparent polar path at the corresponding time. (After Yarger, personal communication, 1984).

The final derived model is shown in figure 30 where the deeper source of mafic intrusion is at mid-crustal depth beneath the MGA. Sedimentary basins of negative density contrast on both sides of the MGA, which have not been suggested by Serpa and others (1984), are also needed in order to match the flanking lows on both sides of the MGA.

The boundary between the Rice formation and granitic basement rocks on the east side of the MGA is determined by drill data. The seismic section of the same area (see figure 7) suggests a gentle west-dipping reflector beneath VP 1400 at time 1.3 s, which can be (imaginatively) traced eastward to the base of Paleozoic strata at about VP 1200 -1250. The reflector may be the base of the arkosic sedimentary basin, as the acoustic properties are expected to change from sedimentary rocks to granitic basement rocks. On the west side of the profile, there is a similar east-dipping reflector beneath VP 2100 at time 2.0 s. This may also be the base of Precambrian sedimentary basin on the west side of the MGA.

The model in figure 30 also suggests that the shallow mafic intrusion at VP 1460 is younger in age than or at least concurrent with the ending of deposition of the eastern Rice formation.

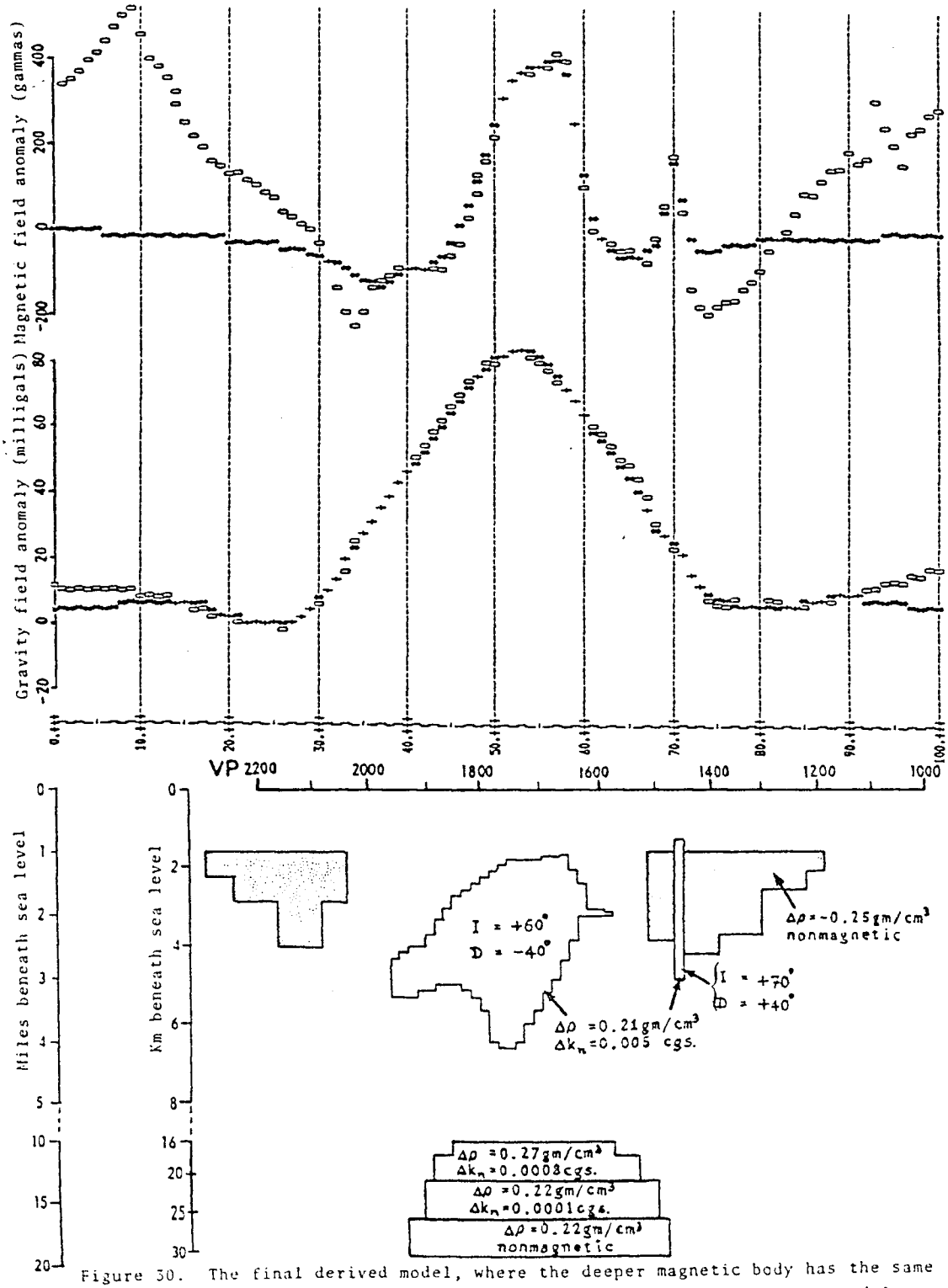

Figure 30. The final derived model, where the deeper magnetic body has the same magnetization direction as the shallow basaltic rift basin model. The horizontal scale is in miles eastward from 98° W longitude. ---------- = Modeled anomaly, oooooooo = Measured anomaly.

The deeper source model of figure 30 requires a small magnetic effect at mid-crustal levels, and becomes nonmagnetic at greater depth. This is possibly related to a high temperature, near or above the Curie point, at great depth. The small magnetic effects of the deeper source may also be due to the extreme low susceptibility contrast corresponding to the magnetic complexity of deep crust, or to the reversed polarity within part of the deep source rock resulting in cancellation of its magnetic effect.

The presence of deeper mafic intrusion beneath the rift basin is originally required to match the gravity anomaly. Deep seismic sections indicate the absence of numerous mid-crustal reflections and diffractions beneath the MGA (Serpa and others, 1984). The seismic quiet zone may be caused by the strong reflection of energy at layered reflectors in the upper crust, resulting in weak energy penetration to deeper crust. However, a few reflections and diffractions still appear in parts of the seismic quiet zone. Therefore, this abnormally quiet zone at mid-crustal depth is possibly related to the mafic intrusion required by the gravity modeling beneath the rift basin.

The observed magnetic profile in figure 30 shows the lows at VP 1400 and VP 2050 on the east and west

sides of the MGA, respectively. Such lows may be due to the extreme depth to the magnetic basement according to the overlying basin of nonmagnetic Rice formation, or the edge effect of other anomalous body beyond both sides of the MGA, or both.

CONCLUSION

In this study, correlations of different geophysical data (gravity, aeromagnetic, and seismic reflection data) and drill data were used to derive a geophysical model of the MGA.

An asymmetric basin filled with interbedded basaltic and clastic rocks, interpreted from the COCORP seismic sections (Serpa and others, 1984), is mainly responsible for the primary positive magnetic anomaly of the MGA due to the high magnetite content of basaltic lava in the shallow crust. The significant remnant magnetization with a Q value of 1, derived from the magnetic modeling, is in accordance with magnetization measurement of Keweenawan mafic rocks in the Northern Region (Jahren, 1965) which reported remnant magnetization to be an important factor.

The deeper mafic intrusion, at midcrustal levels and extending to the deep crust, is required in order to match the positive gravity anomaly. The absence of numerous mid-crustal reflections and diffractions in the seismic sections may be related to this anomalous material. According to magnetic modeling, the intrusive body at midcrustal levels has only a slight magnetic effect which adds to the anomaly amplitude. At greater depth, it becomes nonmagnetic due to the high

temperature, probably near or above the Curie point, or to a poor susceptibility contrast with surrounding rocks, or the polarity reversal within parts of the sources.

The presence of Rice basins on both sides of the MGA is proposed to fit the flanking lows of the gravity anomaly. Basement well cuttings reveal abundant Precambrian sedimentary rocks in this zone. There is seismic evidence, possibly related to the base of sedimentary basin, where the seismic reflections are gently dipping toward the center of the central mafic rift basin. The magnetic second vertical derivative map also shows the magnetic quiet zone on both sides of the MGA to the same extent.

Reprocessing part of COCORP seismic data in the area of the secondary magnetic high, and magnetic modeling, reveal a possible mafic intrusion near the Precambrian basement surface where mafic wells are encountered. The intrusion is a later event, after deposition of the Rice formation, as evidenced by the cross-cutting relationship. Its magnetization direction suggests it occurred in a different ambient earth's magnetic field than the field the basaltic rift basin was formed. Paleopole studies support the younger age of this mafic intrusion.

APPENDIX I

Calculation of the Gravity and Magnetic Fields of a Homogeneous Rectangular Prism

Consider the three-dimensional Cartesian coordinate system with the positive x'-axis to the north, the positive y'-axis to the east, and the positive z'-axis downward (see figure I-1). The profile of calculation is along the y'-axis, ie. the observation point is $(0,y',0)$. The rectangular prism of interest, beneath the $x'y'$-plane, is oriented such that its upper and lower faces are horizontal at depth d_u and d_l , respectively, below the level of observaton. The long axis of a prism rotates clockwise from the north with an angle θ. Its length and width are a and b, respectively.

The computing iterations are as follows.

i) Translation of coordinates along the y'-axis so that the new origin is directly over the center of the east-west width of a prism.

ii) Rotation of coordinates, clockwise from the north with an angle θ, so that the new x- and y- axes are parallel to the vertical sides of a prism (see figure I-1).

iii) Calculation of the gravity and magnetic fields due to a prism in the new coordinates system according to formulae (1) and (2) given below, respectively, ie.

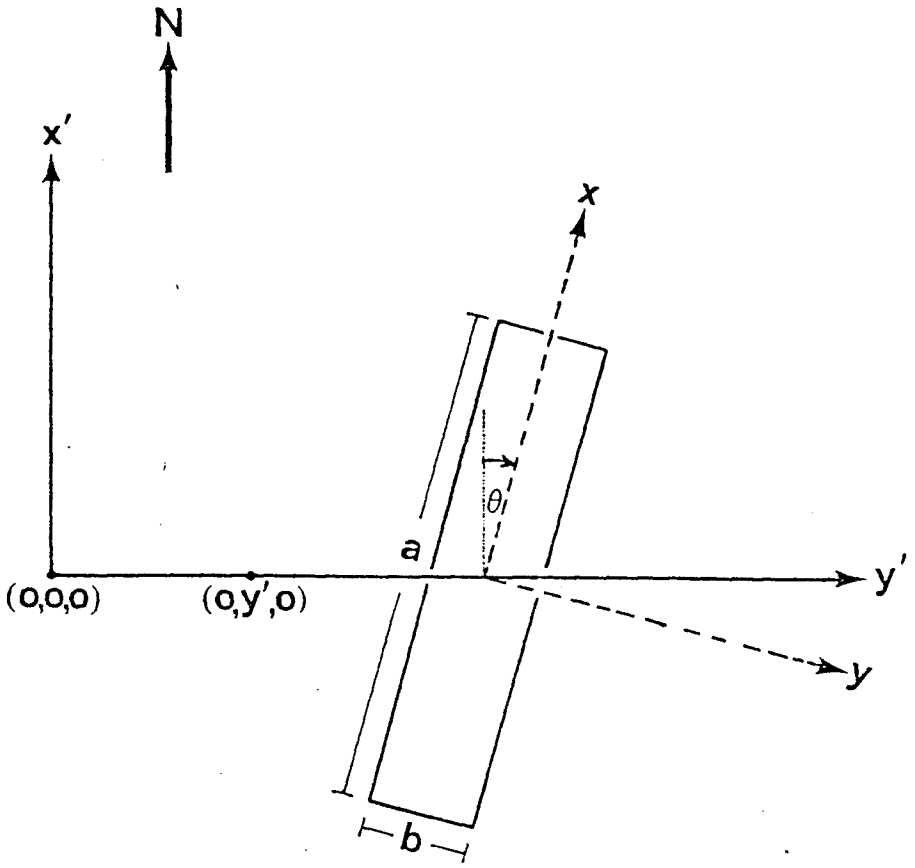

Figure I-1. Plan view showing an east-west profile of calculation along the y'-axis above the rectangular prism. The long axis of a prism makes an angle θ clockwise from the north.

the observation point is (x,y,0) corresponding to this new coordinate system (see figure I-2).

iv) Calculation for the next observation point along the y'-axis in figure I-1 is done by repeating steps i) to iii) above.

According to the coordinate system of figure II-2, the vertical component of gravitational attraction due to a prism of homogeneous density ρ at an observation point (x,y,0), as expressed in equation 3 of Goodacre (1973), is

$$g_z(x,y,0) = -G\rho \left|\left|\left| \alpha \ln[\beta + (\alpha^2+\beta^2+\gamma^2)^{\frac{1}{2}}] + \beta \ln[\alpha + (\alpha^2+\beta^2+\gamma^2)^{\frac{1}{2}}] - \gamma \tan^{-1} \frac{\alpha\beta}{\gamma(\alpha^2+\beta^2+\gamma^2)^{\frac{1}{2}}} \right|\right|\right|_{\alpha=x-(-\frac{a}{2})}^{\alpha=x-\frac{a}{2}} \Bigg|_{\beta=y-(-\frac{b}{2})}^{\beta=y-\frac{b}{2}} \Bigg|_{\gamma=-d_l}^{\gamma=-d_u} \quad (1)$$

where

G is the gravitational constant,

α, β, and γ are coordinates of volume element,

and the minus sign accounts for the attraction.

Let the direction of the earth's magnetic field be specified by the direction cosines l, m, and n; and the direction of the net magnetization vector of a prism, L, M, and N, according to the coordinate system of figure

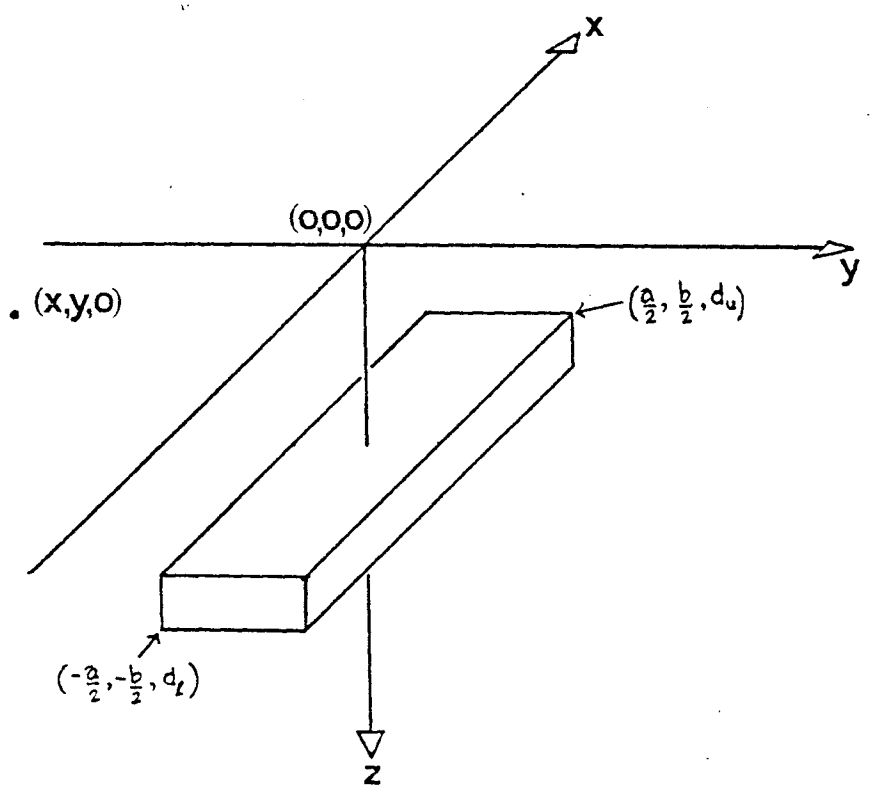

Figure I-2. A rectangular prism with its horizontal upper and lower faces at depth d_u and d_ℓ, respectively, beneath the level of observation on the xy-plane. Its length and width are a and b, respectively.

I-2. The intensity of the total magnetic field due to a prism of net magnetic susceptibility k, measured in the earth's field direction, according to Bhattacharyya (1964)'s equation 10, is

$$F(x,y,o) = kH \left|\left|\left| \frac{(Mn+Nm)}{2} \ln\left(\frac{r_o-\alpha_1}{r_o+\alpha_1}\right) \right.\right.\right.$$

$$+ \frac{(Ln+N\ell)}{2} \ln\left(\frac{r_o-\beta_1}{r_o+\beta_1}\right) - (Lm+M\ell) \ln(r_o+\gamma)$$

$$- L\ell \tan^{-1}\left(\frac{\alpha_1\beta_1}{\alpha_1^2+r_o\gamma+\gamma^2}\right) - Mm \tan^{-1}\left(\frac{\alpha_1\beta_1}{r_o^2+r_o\gamma-\alpha_1^2}\right)$$

$$+ Nn \tan^{-1}\left(\frac{\alpha_1\beta_1}{r_o\gamma}\right) \Bigg|_{\alpha=-\frac{a}{2}}^{\alpha=\frac{a}{2}} \Bigg|_{\beta=-\frac{b}{2}}^{\beta=\frac{b}{2}} \Bigg|_{\gamma=d_\ell}^{\gamma=d_u} \qquad (2)$$

where

$\alpha_1 = \alpha - x$,

$\beta_1 = \beta - y$,

$r_o^2 = \alpha_1^2 + \beta_1^2 + \gamma^2$,

and H is the magnitude of the earth's field (using 56,000 gammas).

APPENDIX II

Reprocessing Parameters of COCORP Seismic Data between VP 1400-1500 and the Upper 3 Seconds of Two-way Travel Time

Sampling rate 8 milliseconds.

1. CDP gather.
2. Datum static: Datum velocity 2600 meter/second
   Datum (line 1) 385 m (above sea level)
   (line 2) 397 m
   (line 3) 417 m
3. Trace equalization window 750 milliseconds.
4. First arrival muting schedule: (line 2)

CDP 2908	Time(ms)	Distance(m)
	0	0
	400	1660
	540	1950
	800	2000
	1100	2570
	1700	3950
	3000	8720

5. Stacking velocity:

		Time(ms)	Velocity(m/s)
Line 1,	CDP 2810	0	3750
		460	4000
		1560	5250
	CDP 2885	0	3750
		450	4000
		1220	5000
		1800	5500
Line 2,	CDP 2905	0	4250
		640	4250
		910	5000
		1800	5600
		2050	5650
Line 3,	CDP 2950	0	3750
		420	4000
		900	5000
		1890	5200
	CDP 2975	0	3750
		430	4000
		1300	5100
		2100	5400

6. Normal moveout.
7. Stack.
8. Filter: bandpass 4-8-32-50 Hz.

BIBLIOGRAPHY

Bhattacharyya, B.K., 1964, Magnetic anomalies due to prism-shaped bodies with arbitrary polarization: Geophysics, v. 29, no. 4, p. 517-531.

Bickford, M.E., Harrower, K.L., Nusbaum, R.L., Thomas, J.J., and Nelson, G.E., 1979, Preliminary geologic map of the Precambrian basement rocks of Kansas: Kansas Geol. Survey Map M-9, scale 1:500,000, 1 sheet.

Bickford, M.E., Harrower, K.L., Nusbaum, R.L., Thomas, J.J., Nelson, G.E., and Hoppe, W.J., 1981, Rb-Sr and U-Pb and geochronology and distribution of rock types in the Precambrian basement of Missouri and Kansas: Geol. Soc. Am. Bull., part 1, v. 92, p. 323-341.

Brookins, D.G., 1970, Kimberlites of Riley County: Kansas Geol. Survey Bull. 200, 32 p.

Brown, L., Serpa, L., Setzer, T., Oliver, J., Kaufman, S., Lillie, R., Steiner, D., and Steeples, D., 1983, Intra-crustal complexity in the U.S. midcontinent: Preliminary results from COCORP surveys in northeastern Kansas: Geology, v. 7, p. 25-30.

Chase, C., and Gilmer, T., 1973, Precambrian plate tectonics: The midcontinent gravity high: Earth and Planetary Sci. Lett., v. 21, p. 70-78.

Chelikowsky, J.R., 1972, Structural geology of the Manhattan, Kansas, area: Kansas Geol. Survey Bull. 204, part 4, 13 p.

Cole, V.B., 1976, Configuration of the top of the Precambrian rocks in Kansas: Kansas Geol. Survey Map M-7, scale 1:500,000, 1 sheet.

Dobrin, M.B., 1976, Introduction to geophysical prospecting, 3rd edition, McGraw-Hill, Inc., 630 p.

Goodacre, A.K., 1973, Some comments on the calculation of the gravitational and magnetic attraction of a homogeneous rectangular prism: Geophys. Prospecting Jour., v. 21, p.66-69.

Hahn, R.K., 1980, Upper mantle velocity structure in eastern Kansas from teleseismic P-wave residuals: M.S. Thesis, Department of Geology, University of Kansas, 85 p.

Halls, H.C., 1966, A review of the Keweenawan geology of the Lake Superior region: in The Earth Beneath the Continents, Steinhart, J.S., and Smith, T.J., eds., Am. Geophys. Union, Geophys. Monogr. no. 10, Washington, D.C., p. 3-27.

Halls, H.C., 1978, The late Precambrian central North American rift system - A survey of recent geological and geophysical investigation: in Tectonics and Geophysics of Continental Rifts, Ramberg, I.B., and Neumann, E.R., eds., D. Reidel Publ., p. 111-123.

Irving, E., 1979, Paleopoles and paleolatitudes of North America and speculations about displaced terrains: Canadian Jour. of Earth Sciences, v. 16, p. 669-694.

Jahren, C.E., 1965, Magnetization of Keweenawan rocks near Duluth, Minnesota: Geophysics, v. 30, no. 5, p. 858-874.

Jewett, J.M., 1941, The geology of Riley and Geary Counties, Kansas: Kansas Geol. Survey Bull. 39, 164 p.

King, E.R., and Zietz, I., 1971, Aeromagnetic study of the midcontinent gravity high of the Central United States: Geol. Soc. America Bull., v. 82, p. 2187-2208.

Lui, C.Y., 1980, Microearthquakes in Red Willow County, Nebraska: M.S. Thesis, Department of Geology, University of Kansas, 53 p.

Mayne, W.H., 1962, Common reflection point horizontal data stacking techniques: Geophysics, v. 27, p. 927-938.

Merriam, D.F., 1963, The geologic history of Kansas: Kansas Geol. Survey Bull. 162, 317 p.

Miller, R.D., 1983, Crustal study in Kansas using earthquake seismograms: M.S. Thesis, Department of Physics, University of Kansas, 105 p.

Ocola, L.C., and Meyer, R.P., 1973, Central North American rift system:1. Structure of the axial zone from seismic and gravimetric data: Jour. Geophys. Res., v. 78, p. 5173-5194.

Schilt, S., Oliver, J., Brown, L., Kaufman, S., Albaugh, D., Brewer, J., Cook, F., Jensen, L., Krumhansl, P., Long, G., and Steiner, D., 1979, The heterogeneity of the continental crust: results from deep crustal seismic reflection profiling using the Vibroseis technique: Reviews of Geophys. and Space Physics, v. 17, p. 354-368.

Scott, R.W., 1966, New Precambrian (?) formation in Kansas: AAPG Bull., v. 50, p. 380-384.

Serpa, L., Setzer, T., Farmer, H., Brown, L, Oliver, J., Kaufman, S., Sharp, J., and Steeples, D., 1984, Structure of the southern Keweenawan rift from COCORP surveys across the Midcontinent Geophysical Anomaly in northeastern Kansas: in press.

Shenkel, C.W., Jr., 1959, Geology of the Abilene anticline in Kansas: Kansas Geol. Soc. 24th Field Conf. Guidebook, p. 116-128.

Snyder, F.G., 1968, Tectonic history of midcontinent United States: University of Missouri at Rolla Jour., no. 1, p. 65-77.

Steeples, D.W., 1976, Preliminary crustal model for northwest Kansas (abstract): EOS (Am. Geophys. Union Trans.), v. 57, no. 12, p. 961.

Steeples, D.W., 1982, Structure of the Salina-Forest City interbasin boundary from seismic studies: University of Missouri at Rolla Jour, no. 3, p. 55-81.

Steeples, D.W., and Bickford, M.E., 1981, Piggyback drilling in Kansas: An example for the continental scientific drilling program: EOS (Am. Geophys. Union Trans.), v. 62, no. 18, p. 473-476.

Steeples, D.W., DuBois, S.M., and Wilson, F.W., 1979, Seismicity, faulting and geophysical anomalies in Nemaha County, Kansas: Relationship to regional structures: Geology, v. 7, p. 134-138.

Steeples, D.W., Rothe, G.H., and Knapp, R.W., 1983, Kansas and Nebraska microearthquakes - 1981-82: Earthquake Notes, v. 54, no. 2, p. 49-55.

Telford, W.M., Geldart, L.P., Sheriff, R.E., and Kays, D.A., 1976, Applied Geophysics: Cambridge University Press, 860 p.

White, W.S., 1966, Tectonics of the Keweenawan basin, Western Lake Superior Region: in Shorter Contributions to General Geology, Geol. Survey Professional Paper 524-E, p. E1-E23.

Yarger, H.L., 1981, Aeromagnetic survey of Kansas: EOS (Am. Geophys. Union Trans.), v. 62, no. 17, p. 173-178.

Yarger, H.L., 1983, Regional interpretation of Kansas aeromagnetic data: Kansas Geol. Survey Geophys. Series, no. 1, 35 p.

Yarger, H.L., and Jarjur, S.Z., 1972, Gravity and magnetic survey of an abandoned lead and zinc mine in Linn County, Kansas: Kansas Geol. Survey Bull. 204, part 2, 13 p.

Yarger, H.L., and Lam, G., 1982, Gravity measurement in Kansas: in Assessment of the Geothermal Resources of Kansas, Department of Energy Report, p. 220-232.

Yarger, H.L., Ng, K., Robertson, R., and Woods, R., 1980, Bouguer gravity map of northeastern Kansas: Kansas Geol. Survey, scale 1:500,000, 1 sheet.

Yarger, H.L., Robertson, R, Martin, J., Ng, K., Sooby, R., and Wentland, R., 1981, Aeromagnetic map of Kansas: Kansas Geol. Survey Map M-16, scale 1:500,000, 1 sheet.

Yarger, H.L., Robertson, R.R., and Wentland, R.L., 1978, Diurnal drift removal from aeromagnetic data using least squares: Geophysics, v. 46, no. 6, p. 1148-1156.